Two-year continuous measurements of carbonaceous aerosols in urban Beijing, China: temporal variations, characteristics and source analyses

Dongsheng Ji[1*], Yingchao Yan[1, 2], Zhanshan Wang[3], Jun He[4], Baoxian Liu[3], Yang Sun[1], Meng Gao[5], Yi Li[6], Wan Cao[1, 2], Yang Cui[1, 2], Bo Hu[1], Jinyuan Xin[1], Lili Wang[1], Zirui Liu[1], Guiqian Tang[1], Yuesi Wang[1*]

[1] *State Key Laboratory of Atmospheric Boundary Layer Physics and Atmospheric Chemistry, Institute of Atmospheric Physics, Chinese Academy of Sciences, Beijing, China*

[2] *University of Chinese Academy of Sciences, Beijing, China*

[3] *Beijing Municipal Environmental Monitoring Center, Beijing, China*

[4] *Natural Resources and Environment Research Group, International Doctoral Innovation Centre, Department of Chemical and Environmental Engineering, University of Nottingham Ningbo China, Ningbo, China*

[5] *John A. Paulson School of Engineering and Applied Sciences, Harvard University, Cambridge MA, USA*

[6] *Arizona Department of Environmental Quality, Phoenix, AZ, USA*

* Corresponding author

Email address: jds@mail.iap.ac.cn; wys@dq.cern.ac.cn

Abstract

Organic carbon (OC) and elemental carbon (EC) in the $PM_{2.5}$ of urban Beijing were measured hourly with a semi-continuous thermal-optical analyzer from Jan 1, 2013 to Dec 31, 2014. The annual average OC and EC concentrations in Beijing were 17.0±12.4 and 3.4±2.0 μg/m^3 for 2013, and 16.8±14.5 and 3.5±2.9 μg/m^3 for 2014. It is obvious that the annual average concentrations of OC and EC in 2014 were not less than those in 2013 while the annual average $PM_{2.5}$ concentration (89.4 μg/m^3) in 2014 was slightly reduced as compared to that (96.9 μg/m^3) in 2013. Strong seasonality of the OC and EC concentrations were found with high values during the heating seasons and low values during the non-heating seasons. The diurnal cycles of OC and EC characterized by higher values at night and in the morning were caused by primary emissions, secondary transformation and stable meteorological condition. Due to increasing photochemical activity, the OC peaks were observed at approximately noon. No clear weekend effects were observed. Interestingly, in the early mornings on weekends in the autumn and winter, the OC and EC concentrations were close to or higher than those on weekdays. Our data also indicate that high OC and EC concentrations were closely associated with their potential source areas which were determined based on the potential source contribution function analysis. High potential source areas were identified and were mainly located in the south of Beijing and the plain of northern China. A much denser source region was recorded in the winter than in the other seasons, indicating that local and regional transport over regional scales are the most important. These results demonstrate that both regional transport from the southern regions and local accumulation could lead to the enhancements of OC and EC and likely contribute to the severe haze pollution in Beijing.

Keywords OC, EC, $PM_{2.5}$, Beijing, Meteorological effects

1. Introduction

Organic carbon (OC) and elemental carbon (EC) represent major fractions of $PM_{2.5}$ and play important roles in the states of human health, the atmospheric environment and climate change (Bond et al., 2013; World Health Organization, 2005; Seinfeld and Pandis, 2016; IPCC AR5, 2013). Epidemiologic studies illustrate the risks of exposure to these particles by showing that the increasing levels of OC and EC in urban areas were closely associated with cardiovascular mortality and morbidity (Pope et al., 2006; Mauderly et al., 2008). In addition, OC, which includes polycyclic aromatic hydrocarbons (PAHs) and polychlorinated biphenyls (PCBs), has the potential to induce carcinogenic and mutagenic effects, while EC, which includes mediums carrying heavy metals and PAHs, has adverse effects on public health (Biswas et al., 2009). In addition to health risks, OC, EC and the mixing of OC and EC with anthropogenic inorganic constituents have been shown to result in the degradation of air quality and visibility impairments (Ji et al., 2017). Furthermore, OC and EC have significant effects on the Earth radiation balance and, in turn, on the climate at both global and regional scales through direct and indirect radiative forcing. OC and EC also play key roles in the formation of cloud condensation nuclei, resulting in higher albedos of cloud and more intense monsoon circulation and rainfall patterns (Bond et al., 2013). Therefore, worldwide attention has been paid to studies of OC and EC. In particular, there is greater concern regarding the high emissions of OC and EC in rapidly developing countries.

High loadings of OC and EC have been recorded in China for decades (Lu et al., 2011; Pan et al., 2011, 2013). As one of the most developed agglomerations in China, the Beijing-Tianjin-Hebei (BTH) region is heavily influenced by anthropogenic emissions, resulting in severe air pollution

(Zhao et al., 2013). A series of field measurements of OC and EC were carried out in the North Plain of China, including in Beijing, Tianjin and Hebei province (Cheng et al., 2013; Ji et al., 2014, 2016; Andersson et al., 2015). As reported by Yao et al. (2014), spatial differences in the OC and EC occurrence levels were found in the BTH region, and high concentrations were observed in the autumn and winter. He et al. (2001) presented the concentrations of OC and EC in $PM_{2.5}$ and found that carbonaceous aerosols (CAs) are the main components of $PM_{2.5}$ in Beijing. Ji et al. (2016) concluded that clean energy strategies led to effective declines in the OC and EC concentrations, and high concentrations of secondary organic carbon (SOC) were observed in the autumn and winter. The previous studies of OC and EC were mainly based on filter sampling for multiple hours or several days and on subsequent laboratory analyses, all of which are susceptible to sampling and analysis artifacts (uncertainty of the artificial sampling was relative larger.) (Cheng et al., 2011). Additionally, the low temporal-resolved results can mask detailed variations and characteristics of OC and EC. Yearly high-temporal-resolution studies of OC and EC are invariably scarce (Lin et al., 2009; Zhao et al., 2013; Ji et al., 2016; Chang et al., 2017). It is therefore necessary to study the variation, accumulation and transport of OC and EC as well as the relationship between OC and EC to understand the processes and sources affecting the evolution of OC and EC based on high-time resolved continuous in situ measurements.

Most of previous studies were conducted before the implementation of the Air Pollution Prevention and Control Action Plan in September 2013. After the execution of this action plan, air quality improved in Beijing, with the annual mean $PM_{2.5}$ concentrations declining from 96.9 in 2012 to 89.4 $\mu g/m^3$ in 2013. Although a decline in the $PM_{2.5}$ concentrations was observed, the annual mean $PM_{2.5}$ concentrations were still much higher than the secondary Chinese annual mean

89 $PM_{2.5}$ standard (35 μg/m^3) and the World Health Organization's annual-average guideline for
90 $PM_{2.5}$ (15 μg/m^3). Considering that OC and EC account for high fractions of $PM_{2.5}$ (He et al., 2001,
91 2011; Cao et al., 2004) and are closely associated with fuel combustion, thus, scientific knowledge
92 of OC and EC is a prerequisite for effectively establishing and enforcing preventative and
93 corrective measures concerning fossil fuel consumption-related emissions as well as for finally
94 attaining both national and international $PM_{2.5}$ standards. However, the effectiveness of emission
95 abatement and pollution control measures on ambient OC and EC have seldom been analyzed in
96 Beijing in detail.

97 In the present study, two-year hourly OC and EC concentrations were observed using a
98 semi-continuous OC/EC analyzer in the central zone of Beijing from Jan 1, 2013, to Dec 31, 2014.
99 To the best of our knowledge, this was the comprehensive study of OC and EC in the urban core
100 area of Beijing based on continuous two-year-long hourly time-resolved OC, EC, $PM_{2.5}$ and
101 meteorological parameter data. This work was part of the campaign sponsored by the Strategic
102 Priority Research Program of the Formation, Mechanism and Control Strategies of Haze in China,
103 launched by the Chinese Academy of Sciences (CAS). One of the purposes of this program was to
104 better understand the characteristics of the chemical compositions of $PM_{2.5}$ in China and to
105 evaluate the efficiencies of air pollution control measures for air quality improvement. In addition,
106 the strictest air pollution control measures were implemented during the study period, and a
107 comparative analysis was carried out between the pre- and post-implementation states of these
108 measures as energy structure and policy were expected to change significantly. The OC and EC
109 characteristics and their seasonal and diurnal variations are discussed. Finally, the potential source
110 areas contributing to the high concentrations of OC and EC during the four seasons are analyzed

using potential source contribution function (PSCF) analysis.

2. Experiments

2.1 Measurement site

As shown in Fig. 1, the sampling point (39°55′38″ N, 116°19′29″ E, 40 m Alt) surrounded by residential areas and without any nearby industrial source is a typical urban site in the central zone of Beijing. It is located approximately 1.2 km away from the west 3rd Ring Road and 2.7 km away from the north 2nd Ring Road. Both ring roads are characterized by heavy traffic (http://www.bjtrc.org.cn/JGJS.aspx?id=5.2&Menu=GZCG), and their annual-average vehicular speeds during the morning (7:00-9:00) and evening traffic peaks (17:00-19:00) were 27.4 and 24.2 km/h and 27.8 and 23.2 km/h in 2013 and 2014, respectively. The sampling campaign was conducted from January 1, 2013 to December 31, 2014.

As shown in Fig. S1(a), obvious seasonal distributions were recorded for the atmospheric temperature (*T*), relative humidity (*RH*), wind speed (*WS*) and direction (*WD*), atmospheric pressure (*P*), UV radiation (*UV*), precipitation (*Prec.*) and mixed layer height (MLH). The monthly average RH was higher than 50 % in the summer and reached its minimum value (approximately 30 %) in the spring. *T* and *UV* showed similar seasonal cycles characterized by low values in the winter and high values in the summer. The monthly variations of WS varied from 1.0 to 2.0 m/s, with slightly higher values in the spring. In addition, the rainy season lasted from June to September, while precipitation was almost negligible during the wintertime.

2.2 Instrumentation

Hourly OC and EC concentrations of $PM_{2.5}$ were recorded using a OC/EC analyzer (Model 4, Sunset Laboratory Inc. Oregon, USA) with the thermal-optical transmission method. Volatile

organic compounds were removed by inline parallel carbon denuder removing installed on the analyzer. Round 16-mm quartz filters were used for collecting OC and EC samples at a sampling flow rate of 8 L/min. OC and EC samples were collected for 40 minutes and then were analyzed in approximately 15 minutes. The multiple programmed steps were based on the NIOSH 5040 thermal protocol, which has been introduced by Cassinelli et al. (1998). A non-dispersive infrared (NDIR) detector was used for quantifying particulate OC and EC concentrations. For the charring correction, the sample transmittance was recorded by a He-Ne laser beam (665 nm wavelength) system throughout the analysis process. The split point between OC and EC was obtained when the transmittance of laser signal returned to its initial value (Birch et al., 1996). The standard procedure for calibration has been introduced in manual of the OC and EC analyzer in details (https://www3.epa.gov/ttnamti1/files/ambient/pm25/spec/Sunset_Manual.pdf). The quartz fiber filters used for sampling was changed when the laser correction factor drops below 0.90. An instrument blank was conducted when the quartz fiber filters was changed. An internal standard CH_4 mixture (5.0 %; ultrahigh purity He balance) was used to calibrate the analyzer automatically at the end of every analysis. In addition, an off-line calibration was performed using an external source of sucrose standard (2.06 g/L) every three months. The range of total carbon (TC, a sum of OC and EC) for the NIOSH protocol varies from 0.7 to 70 μg C/cm^2 and the limit of detection (LOD) is calculated at 0.15 μg C/cm^2 (Birch and Cary, 1996; Peterson and Richards, 2002). It might be negligible for $PM_{2.5}$ to overestimate OC or EC caused by CC interference due to the contribution of CC in $PM_{2.5}$ less than 5 % of TC.

Ambient $PM_{2.5}$, O_3, SO_2 and NO_2 were measured using a tapered element oscillating microbalance $PM_{2.5}$ monitor with a Filter Dynamics Measurement System (Model 1405,

Thermo-Fisher Scientific (TE)), a UV photometric O_3 analyzer (Model 49i, TE), a pulsed fluorescence SO_2 analyzer (Model 43i, TE) and a chemiluminescence NO-NO_2-NO_x analyzer (Model 42i, TE), respectively. Detailed information on the ambient $PM_{2.5}$, O_3, SO_2 and NO_2 analyzers has been reported by Ji et al. (2014). The SO_2 and NO_2 analyzers were calibrated using a 50 ppmv SO_2 standard gas and a 52 ppmv NO standard gas (Scott-Marrin gases, Riverside, CA, USA), respectively. In addition, an O_3 calibrator (49I PS, TE), which can be traceable to the standard reference photometer at the US National Institute of Standards and Technology, was used to calibrate the O_3 analyzer. The CO concentrations at the Dingling station (issued by website, http://zx.bjmemc.com.cn/getAqiList.shtml?timestamp=1507517944788) were selected as the $CO_{background}$ concentrations.

Hourly data of atmospheric temperature (*T*), relative humidity (*RH*), ultraviolet radiation (*UV*), wind speed (*WS*) and direction (*WD*), precipitation (*Prec.*) and mixed layer height (MLH), were downloaded from the meteorological tower of the Institute of Atmospheric Physics (IAP), CAS during the sampling periods.

2.3 PSCF analysis

Potential source contribution function (PSCF) analysis can be used to identify possible source areas affecting air pollution levels. In principle, PSCF uses backward trajectories to determine potential locations of emission sources. The PSCF is defined as:

$$\mathrm{PSCF}(i,j) = W_{ij} \times (m_{ij}/n_{ij}) \quad (1)$$

where n_{ij} is the total number of back-trajectory segment endpoints that fall into the grid cell (i, j), n_{ij} is the number of points with concentrations of air pollutants higher than a threshold value (m_{ij}) and W_{ij} is an empirical weight function proposed to reduce the uncertainty of n_{ij} during the study

period. Higher ratios of m_{ij}/n_{ij} illustrate higher probability of particular grids through which passing air masses will lead to higher receptor concentrations.

The National Oceanic and Atmospheric Administration Hybrid Single-Particle Lagrangian Integrated Trajectory model (HYSPLIT 4.9) were used for calculating the 48 h backward trajectories terminating at the study site at a height of 100 m every 1 hour during the sampling period (Draxler and Rolph, 2003). In this study, the domain for the PSCF was set in the range of (30-60 °N, 65-150 °E). The 75th percentile for OC and EC for each season was used as the threshold values to calculate m_{ij}. A weighting function (w_{ij}) introduced by Wang et al. (2009) and Polissar et al. (1999) was used in the PSCF to reduce the uncertainties for those grid cells with a limited number of points in each season of 2013 and 2014.

3. Results and discussion

3.1 Occurrence levels of OC and EC

The distributions of OC and EC at the urban sampling site in Beijing from 2013 to 2014 are presented in Fig. 2. As shown in Fig. 2, the hourly OC concentrations ranged from 1.1 to 143.1 μg/m^3 and from 0.3 to 135.1 μg/m^3 with averages of 17.0 ± 12.4 μg/m^3 and 16.8 ± 14.5 μg/m^3 in 2013 and 2014, respectively. In addition, the EC concentrations ranged from 0.2 to 28.1 and from 0.2 to 31.7 μg/m^3 with averages of 3.4 ± 2.0 μg/m^3 and 3.5 ± 2.9 μg/m^3, respectively. The average OC concentration was higher than that (14.5±12.1 μg/m^3) observed at the IAP site located between the north 3rd Ring and 4th Ring roads in urban Beijing (shown in Fig. 1), while the average EC concentration was lower than that (4.4±4.0 μg/m^3) observed at the IAP site. In contrast to the results observed at the IAP site, the OC/EC ratios were 6.6±4.5 and 6.5±3.2 in 2013 and 2014, respectively, which were higher, suggesting the spatial differences in the emissions of

OC and EC in urban Beijing.

The contributions of OC and EC to the measured $PM_{2.5}$ mass concentrations were averagely 17.6 and 3.5 %, respectively, in 2013 and 18.8 and 4.0 % in 2014. OC accounted for 83.3 ± 8.5 and 82.6±7.4 % of the TC for these two years, indicating that OC was the predominant carbon contributor. In this study, the contributions of TC to $PM_{2.5}$ were found to be 21.1 ± 19.1 and 22.7 ± 29.9 % in 2013 and 2014, respectively, which were similar with those reported in Beijing's 2012 Environmental Status (e.g., the contributions of TC to $PM_{2.5}$ accounted for approximately 21.6 %). The carbonaceous aerosol levels were estimated as the sum of the OC multiplied by 1.4 and the EC concentrations, which accounted for 28.0 ± 26.7 and 30.2 ± 41.9 % of the recorded $PM_{2.5}$ values in 2013 and 2014, respectively, suggesting that the carbonaceous fraction could contribute significantly to the fine particles. The variations of the concentrations and ratios of OC and EC varying with the incremental $PM_{2.5}$ concentrations were also discussed. As shown in Figs. S2(a) and S2(b), Beijing experienced different air quality days classified based on the daily $PM_{2.5}$ concentrations in 2013 and 2014, which were defined as excellent ($0<PM_{2.5}\leq35$ μg/m^3), good ($35<PM_{2.5}\leq75$ μg/m^3), lightly polluted (LP, $75<PM_{2.5}\leq115$ μg/m^3), moderately polluted (MP, $115<PM_{2.5}\leq150$ μg/m^3), heavily polluted (HP, $150<PM_{2.5}\leq250$ μg/m^3) and severely polluted (SP, $PM_{2.5}>250$ μg/m^3), respectively. Approximately 50 % of the days were classified as polluted days (days with daily average $PM_{2.5}$ concentrations greater than 75 μg/m^3) in 2013 and 2014 in Beijing. The OC and EC concentrations were significantly enhanced with the increase of $PM_{2.5}$ concentrations. Note that the OC/EC ratios in 2014 declined significantly when air quality became heavily and severely polluted days in contrast to those in 2013. As reported by Schauer et al. (2001, 2002), the OC/EC ratio could suggest the sources of aerosol particles, and such a ratio of

aerosols emitted from coal combustion was higher than that from vehicles. During heavily polluted and severely polluted days, local emissions played dominant roles in the accumulation of aerosol particles because air masses were stagnant (Sun et al., 2014). The significant decrease of the OC/EC ratios could imply that coal combustion might have been banned to a greater extent after the enforcement of the new air pollution control action plan in 2014, while vehicular emission appeared to be more pronounced during heavily and severely polluted days.

3.2 Seasonal characteristics of OC and EC

Fig. 2 depicts the seasonal variations in OC and EC during the study periods. The observed OC concentrations exhibited strong seasonality in both 2013 and 2014. Higher concentrations were found in the heating seasons (from Nov 15 to Mar 15) while lower concentrations were found in the non-heating seasons in Beijing. The average OC concentrations were 23.0 ± 17.6 and 24.5 ± 20.2 μg/m^3 in the heating seasons of 2013 and 2014, respectively, while the OC concentrations were 14.0 ± 7.0 and 13.1 ± 8.3 μg/m^3 in the non-heating seasons of 2013 and 2014, respectively. The extra fossil fuel consumed for heating clearly led to higher emissions of OC during the heating seasons. In addition, the higher OC concentrations observed may also be attributed to secondary formations of increased amounts of OC precursors from extra fuel combustion used for heating through condensation processes during the unfavorable meteorological conditions like low temperatures and wind speed as well as high humidity in the winter (Pandis et al. 1992; Odum et al. 1996). The low temperature is favorable for semi-volatile OC condensed onto existing particles and high RH being conducive to the dissolution of water-soluble gases into liquid aerosol particles are known to result in further chemical reactions within these particles, which contributes to the OC concentrations (Seinfeld and Pandis, 2016).

Additionally, cold starts of vehicles result in significantly higher emissions of carbonaceous particles and their precursors in the winter (Singer et al., 1999). Conversely, high atmospheric temperature result in more VOCs partitioned into the gas phase (Pandis et al., 1992; Odum et al., 1996). In contrast to heating seasons, less fossil fuel is consumed for heating in the non-heating seasons, and the lower OC concentrations were observed in the spring, the summer and most of the autumn. Besides residential heating, other energy consumed by transport and industry was also important OC sources, but these sources almost have no seasonal differences except for in the winter.

In addition to the contributions of sources, different weather conditions also play important roles in the seasonal differences of OC concentrations. In the autumn, the average wind speeds were 1.1 and 1.0 m/s in 2013 and 2014, respectively, which were the lowest of the four seasons. The average pressures were 1,013.4 and 1,013.0 hPa in these two years, respectively, and uniform pressure systems frequently dominated northern China in the autumn. Due to the weak pressure gradient, the meteorological conditions were conducive to air pollutant accumulations, thus, led to high OC concentrations. The highest WS recorded in the spring was conducive to air pollutant dispersion and transport, while the frequent precipitation could remove more air pollutants in the summer. These meteorological conditions resulted in lower OC concentrations in the spring and summer. In addition, the lowest OC concentration observed in the summer was also because high ambient temperatures will help shift the gas-particle partitioning of semi-volatile organic compounds toward the gaseous phase. The differences in OC values between the winter and summer could suggest seasonal variations in emission sources (Zhao et al., 2013). The ratios of OC_{spring}/OC_{summer}, OC_{autumn}/OC_{summer} and OC_{winter}/OC_{summer} were 1.0, 0.8 and 1.6 for 2013 and 1.2,

1.6 and 2.1 for 2014, respectively. To exclude the dispersion effect of the planetary boundary layer (PBL), the ratios of OC/ΔC_{CO} (C_{co}-$C_{co\ background}$, Kleinman et al., 2008) can be widely used for the analyses in this study. The ratio of OC/ΔC_{CO} shows similar seasonal variation with OC concentrations. The ratios of OC/ΔC_{CO} between the winter and summer were 1.07 for 2013 and 1.06 for 2014, respectively, suggesting that fossil fuel used for heating plays an important role in the OC concentrations in urban Beijing and that more efforts to control residential heating emissions are needed to improve air quality in Beijing.

The average EC concentrations in the winter were approximately 1.5 and 2.1 times higher than those in the summers of 2013 and 2014, respectively. Note that the differences in the EC concentrations between the winter and summer were higher than those observed in the north and northwest of the urban center of Beijing before the 2008 Olympic Games (Han et al., 2009). By comparison, effective control of coal consumption and highly polluting vehicles played important roles in the decline in EC concentrations. Moreover, the EC concentrations obviously declined more significantly in the summer than in the winter. As shown in the Beijing statistics yearbook, natural gases and electrical appliance were widely used to replace coal and heavily polluting motorized vehicles were banned (http://www.bjstats.gov.cn/nj/main/2015-tjnj/indexch.htm). In addition, household honeycomb-briquette burning and small stoves for cooking and heating were strictly banned inside the 4th ring of Beijing. This was consistent with the decline in the volume of coal consumption.

Similar to OC, higher EC concentrations in $PM_{2.5}$ were observed in the autumn and winter, while lower levels were recorded in the spring and summer. The highest EC concentrations in $PM_{2.5}$ were recorded in the winter with averages of 4.1±2.2 and 4.9±3.9 μg/m^3 for 2013 and 2014,

287 respectively, which were lower than the previous results observed in the autumn (Hu et al., 2009;
288 Zhao et al., 2013). These observations suggest that improvement of air quality in Beijing through
289 governmental and public efforts were effective in somewhat reducing EC concentrations despite
290 the rapidly multiplying vehicle fleet within the municipality. The average concentrations of EC in
291 the autumn of 2013 and 2014 were approximately 1.3 and 1.9 times higher than those in the
292 summers. Lower occurrence levels of EC (with averages of 2.7 ± 1.7 and 2.1 ± 1.2 μg/m^3 for 2013
293 and 2014, respectively) in the summer could be attributed to favorable meteorological conditions
294 (e.g., strong and frequent precipitation and high MLH height) and low emission intensities.

295 **3.3 Diurnal characteristics of OC and EC**

296 As shown in Fig. 3 (a), the obvious diurnal OC and EC variations were observed in the four
297 seasons in 2013 and 2014. The EC peaks were associated with rush hours, indicating that
298 vehicular emission resulted in these spikes. The EC concentrations remained at high levels from
299 the nighttime to early the next morning, likely due to stable meteorological conditions caused by
300 the decay of PBL (Miao et al., 2016; Guo et al., 2016) and the emissions from both heavy-duty
301 diesel trucks (HDDT) and heavy-duty vehicles (HDV). That is because that HDV and HDDT are
302 allowed to enter urban areas inside the 5th Ring Road from 0:00 to 06:00 (Local Time) by Beijing
303 Traffic Management Bureau (http://www.bjjtgl.gov.cn/Inquiries/roadControl.asp), whereas, at
304 other times, both higher PBL heights and lower EC emission intensities from HDV and HDDT
305 occurred. It was obvious that in the winter large-amplitude variations in the average EC
306 concentrations were recorded. The maximum peak concentrations (0:00-10:00) were 1.4, 1.5, 1.6
307 and 1.8 times higher than those observed in the valley concentrations (13:00-15:00) for the spring,
308 summer, autumn and winter, respectively.

309 The peak diurnal OC patterns were associated with traffic conditions in the four seasons of
310 2013 and 2014. In addition, one small additional peak occurred between 12:00 and 14:00, likely
311 due to the SOC formation caused by increases in solar radiation during midday. Note that the OC
312 peaks occurred from evening traffic rush hour to early the next morning, which can also be caused
313 by the decay of PBL and stronger traffic emissions as discussed for the above EC peak patterns.
314 Note that it was obvious that OC and EC concentrations in the autumn and winter of 2014
315 were higher than or close to those in 2013 while OC and EC concentrations in the spring and
316 summer of 2014 were higher than those in 2013 based on diurnal variations of OC and EC
317 concentrations. The results were similar with the variation of $PM_{2.5}$, showing that the frequent
318 occurrence of severe pollution episode in the autumn and winter was closely associated with the
319 roaring increase in $PM_{2.5}$ concentrations although evident improvement in air quality was
320 observed in the spring and summer. The synergetic effect of high emission, unfavorable
321 meteorological condition and regional transport in the autumn and summer offsetting the air
322 quality betterment in the other two seasons led to no marked decline in annual average
323 concentrations of OC and EC.
324 **3.4 Weekend effects**
325 The weekly cycles of OC and EC are of great interest because they provide insights into how
326 these pollutants respond to changes in anthropogenic emissions on weekdays and weekends. As
327 shown in Fig. 3(b), the diurnal cycles of OC and EC on weekdays and weekends were recorded
328 for 2013 and 2014. Differing from previous studies (Grivas et al., 2012; Jeong et al., 2017), no
329 clear weekend effects were observed. The average OC and EC concentrations on the weekends
330 were 17.5±13.9 and 3.4±2.0 μg/m^3 for 2013 and 16.7±12.0 and 3.6±2.7 μg/m^3 for 2014,

respectively, while those on the weekdays were 16.8±11.8 and 3.4±2.0 μg/m^3 for 2013 and 16.5 ±12.5 and 3.5±3.0 μg/m^3 for 2014, respectively. The average OC and EC concentrations during the weekdays were lower or close to those during the weekends in 2013 and 2014, respectively. In particular, the OC and EC concentrations in the early morning on weekends in the autumn and winter were higher than those on weekdays. This suggests that there is no significant decline in anthropogenic activity in the early mornings from weekdays to weekends. Conversely, enhanced anthropogenic emissions might have occurred in the early mornings on weekends in the autumn and winter. As mentioned above, HDV and HDDT are allowed to operate from 0:00 to 6:00 LT. The enhancement of the OC and EC concentrations could be attributed to enhanced traffic emissions, which are consistent with higher NO_x and CO concentrations (not shown). The above results imply that more strict control of the emissions from HDV and HDDT should be carried out on weekends.

3.5 Source analysis

Fig. 4 shows the relationships between the concentrations of OC and EC and the wind sectors in the different seasons of 2013 and 2014. Higher concentrations of OC and EC frequently occurred when the east (E), northwest (NW) and southerly winds prevailed in the spring and summer, while lower concentrations occurred when the north (N) and northeast (NE) winds prevailed. In the spring, the average OC and EC concentrations from the S were 16.4±6.3 and 3.1 ±1.3 μg/m^3 for 2013 and 12.9±6.2 and 2.5±1.3 μg/m^3 for 2014, respectively, which were approximately 1.1 and 1.3 times and 1.2 and 1.1 times higher than those from the N for 2013 and 2014. However, the OC and EC gradients associated with the different wind sectors in the summer were obviously lower than those in the spring. In the summer, the average OC and EC

353 concentrations from the SE were 15.5±5.7 and 2.7±2.5 μg/m^3 for 2013 and 13.3±4.6 and 2.2±
354 1.3 μg/m^3 for 2014. Higher OC and EC concentrations occurred more frequently as the wind
355 sectors changed along the N–NE–E–SE-S gradient, and then decreased along the S–SW–W-NW
356 gradient. Such a relationship between the wind sectors and the OC and EC concentrations is
357 remarkably consistent with the spatial distributions of $PM_{2.5}$ in northern China in 2013 and 2014
358 (China Environmental Statement, 2013, 2014). These results suggest that differences existed in the
359 air pollution around the study site in the autumn and winter. In fact, the average OC and EC
360 concentrations from the S were 13.3±5.7 and 2.8±1.7 μg/m^3 in the autumn of 2013 and were
361 15.7±4.6 and 3.2±2.6 μg/m^3 in the autumn of 2014, respectively. The winter season showed that
362 the OC and EC concentrations from the southerly wind ranged from 1.8 to 143.1 and 0.2 to 28.1
363 μg/m^3 in 2013 and 0.5 to 135.1 and 0.2 to 31.7 μg/m^3 in 2014, respectively, with OC being the
364 major fraction in $PM_{2.5}$, accounting for an average of 18.0 %.

365 Moreover, higher OC and EC concentrations were recorded when calm wind prevailed (Fig.
366 S1(b)). The relatively high OC and EC concentrations corresponded with southerly wind whereas
367 northerly winds with high speeds were favorable for low OC and EC concentrations. Thus, both
368 the long-range transport and local emissions played important roles in the OC and EC
369 concentrations.

370 A clear visualization of the extent of the regional transport and local emissions can be
371 obtained based on the PSCF results of the hourly resolved input data. As shown in Fig. 5, the
372 potential source areas for OC and EC varied among the four seasons of 2013 and 2014. There
373 were almost no differences in the potential source regions of OC and EC for 2013 and 2014, but
374 slight seasonal differences existed in the potential source regions of OC and EC. In the springs of

2013 and 2014, an obvious high potential source area of OC and EC was observed, located in the southern plain areas of Beijing, including parts of the Hebei, Shandong and Henan provinces. This pattern indicated that anthropogenic emissions from the southern plain areas of Beijing played important roles in the OC and EC concentrations in Beijing because the southern plain areas were heavily polluted areas influenced by high pollutant emissions from rapid economic growth, enhancements in energy consumption and vehicle population growth as well as industrial production.

In contrast to the contributions from the source regions in the spring, OC and EC had slightly smaller potential source regions in the summers of 2013 and 2014, the high potential source areas of OC and EC (>0.4) were also located to the south, southwest, and southeast of Beijing including Tianjin, Hebei and Shandong provinces. The PSCF plots of OC showed slightly different patterns to those of EC, potentially indicating a greater formation of secondary OC from volatile organic compounds from the source regions under high O_x conditions during the transport processes in the summer.

The potential source areas for OC and EC in the autumns of 2013 and 2014 were also similar to those in the spring. A distinct source area to the southeast of Beijing including Tianjin and the Bohai Sea, was also observed. The topography of the North China Plain agreed well with this pollution band, with the Taihang Mountains to the east and the Yan Mountains to the south, in particular for the adjacent areas of the Hebei and Shandong provinces. These results illustrate that regional transport from the south was involved in the formation of the severe air pollution in the autumn.

Large difference in PSCF distributions existed between winter and the other seasons. The high PSCF values were mainly located in the regions including the Hebei province, Tianjin, small parts of the Shanxi province, the Shandong province and Inner Mongolia. This pattern indicates that the cities far from Beijing are likely not very important sources of the wintertime CAs in Beijing. That is likely because stagnant synoptic conditions like low WS and temperature inversions occurred more frequently in the winter. Thus, local emissions and circulation from nearby or surrounding regions would have vital impacts on the pollution levels in Beijing. This result is consistent with those of previous studies, indicating that the transport of OC and EC from the SW to the NE along the Taihang Mountains in North Plain of China has been observed (Wu et al., 2014; Ren et al. 2004). Given that many highly polluted cities were located in this pathway, such as Shijiazhuang (annual average $PM_{2.5}$ value in 2014, 126 μg/m^3), Baoding (annual average $PM_{2.5}$ value in 2014, 129 μg/m^3) and Hengshui (annual average $PM_{2.5}$ value in 2014, 108 μg/m^3), regional transport from these regions would have a potentially high effect on the contributions of OC and EC in Beijing.

4. Conclusions

To understand the characteristics of $PM_{2.5}$-associated OC and EC in urban Beijing and to evaluate the effects of air pollution control measures on air quality improvement, two years of hourly OC and EC concentrations were recorded using a semi-continuous OC/EC instrument in the central zone of Beijing from Jan. 1, 2013 to Dec. 31, 2014. The following conclusions were obtained.

The average OC and EC concentrations were similar in 2013 and 2014. The mass fractions of OC and EC in $PM_{2.5}$ declined when the air quality deteriorated, indicating that inorganic aerosols

might have played more dominant roles in the formation of air pollution in Beijing during this study.

OC and EC showed distinctive seasonal and diurnal variations. The higher concentrations in the winter than those in the summer were largely because of enhanced coal combustion emissions. No clear weekend effects were observed in contrast to developed regions with clear weekly variations, possibly indicating stronger primary emissions in the atmosphere over Beijing. The significant decrease of the OC/EC ratios could imply that vehicular emission appeared to be more pronounced instead of coal combustion during heavily and severely polluted days.

Higher OC and EC concentrations were commonly related with wind from the S, E, and SE. A common high potential source area appeared to focus on the south of Beijing, along the Taihang Mountains in spring, summer and autumn, indicating the potentially high influence of the regional transport on OC and EC concentrations in Beijing. A much smaller source region was identified in the winter than in the other seasons, implying that the accumulations of local emissions and regional transport over smaller regional scales could contribute more significantly to the high air pollution events in the winter. The PSCF analysis clearly showed that stricter controls are needed for further mitigation of air pollution on a regional scale.

Acknowledgment

This work was supported by the National Key Research and Development Program of China (2016YFC0202701) and the Beijing Municipal Science and Technology Project (D17110900150000). The authors would like to thank all of the members of the LAPC/CERN in IAP, CAS, for maintaining the instruments used herein. We would also like to thank NOAA for providing the HYSPLIT and TrajStat model.

Reference

Andersson, A., Deng, J., Du, K., Zheng, M., Yan, C., Sköld. M., Gustafsson, Ö., 2015. Regionally varying combustion sources of the January 2013 severe haze events over eastern china. Environmental Science and Technology 49(4), 2038-2043.

Birch, M., Cary, R., 1996. Elemental carbon-based method for monitoring occupational exposures to particulate diesel exhaust. Aerosol Science & Technology 25(3), 221-241.

Peterson, M. R., Richards, M. H., 2002. Thermal-Optical-Transmittance Analysis for Organic, Elemental, Carbonate, Total Carbon, and OCX2 in $PM_{2.5}$ by the EPA/NIOSH Method. Research Triangle Institute.

Biswas, S., Verma, V., Schauer, J. J., Cassee, F. R., Cho, A. K., Sioutas, C., 2009. Oxidative potential of semi-volatile and non-volatile particulate matter (PM) from heavy-duty vehicles retrofitted with emission control technologies. Environmental Science & Technology 43(10), 3905-3912.

Bond, T. C., Doherty, S. J. Fahey, D. W., Forster, P. M., Berntsen, T., DeAngelo, B. J., Flanner, M. G., Ghan, S., Kärcher, B., Koch, D., Kinne, S., Kondo, Y., Quinn, P. K., Sarofim, M. C., Schultz, M. G., Schulz, M., Venkataraman, C., Zhang, H., Zhang, S., Bellouin, N., Guttikunda, S. K., Hopke, P. K., Jacobson, M. Z., Kaiser, J. W., Klimont, Z., Lohmann, U., Schwarz, J. P., Shindell, D., Storelvmo, T., Warren, S. G., Zender, C. S., 2013. Bounding the role of black carbon in the climate system: A scientific assessment. Journal of Geophysical Research: Atmospheres 118(11), 5380-5552.

Boparai, P., J. Lee, and T. C. Bond, 2008.Revisiting thermal-optical analyses of carbonaceous aerosol using a physical model. Aerosol Science and Technology 42, 930-948.

462 Cao, J., Lee, S., Ho, K., 2003. Characteristics of Carbonaceous Aerosol in Pearl River Delta
463 Region, China during 2001 Winter Period. Atmospheric Environment 37, 1451-1460.
464 Cao, J., Lee, S., Ho, K., 2004. Spatial and seasonal variations of atmospheric organic carbon and
465 elemental carbon in Pearl River Delta Region, China. Atmospheric Environment 38(27),
466 4447-4456.
467 Chang, Y. H., Deng, C. R., Cao, F., Cao, C., Zou, Z., Liu, S. D., Lee, X. H., Li, J., Zhang, G.,
468 Zhang, Y., 2017. Assessment of carbonaceous aerosols in Shanghai, China–Part 1: long-term
469 evolution, seasonal variations, and meteorological effects. Atmospheric Chemistry and
470 Physics 17(16), 9945-9964.
471 Cassinelli, M. E., O'Connor, P. F., 1998. NIOSH Method 5040. NIOSH Manual of Analytical
472 Methods (NMAM), Second Supplement to NMAM. 4th ed. DHHS (NIOSH) Publication,
473 94-113.
474 China Environmental Statement, 2013. http://www.mep.gov.cn/hjzl/zghjzkgb/lnzghjzkgb/201605/
475 P020160526564730573906.pdf
476 China Environmental Statement, 2014. http://www.mep.gov.cn/hjzl/zghjzkgb/lnzghjzkgb/201605/
477 P020160526564151497131.pdf
478 Cheng Y., 2011. Study on the Sampling and Analysis Methods of Carbonaceous Aerosol.
479 http://kns.cnki.net/KCMS/detail/detail.aspx?dbcode=CDFD&dbname=CDFD1214&filename
480 =1012035910.nh&v=MDQ1NzJyNUViUElSOGVYMUx1eFlTN0RoMVQzcVRyV00xRnJD
481 VVJMMmVadWR0RnlqbFc3M01WRjI2SExPN0c5ak4=
482 Cheng, Y., Engling, G., He, K. B., Duan, F. K., Ma, Y. L., Du, Z. Y., Liu, J. M., Zheng, M., Weber,
483 R. J., 2013. Biomass burning contribution to Beijing aerosol. Atmospheric Chemistry and

484 Physics 13, 7765–7781.
485 Chow, J., Watson, J., Pritchett, L., Pierson, W., Frazier, C., Purcell, P., 1993. The DRI
486 thermal/optical reflectance carbon analysis system: Description, evaluation and applications
487 in US air quality studies. Atmospheric Environment Part A 27(8), 1185-1201.
488 Draxler, R. R., & Rolph, G. D., 2003. HYSPLIT (HYbrid Single-Particle Lagrangian Integrated
489 Trajectory). NOAA Air Resources Laboratory, Silver Spring, MD. Model access via NOAA
490 ARL READY Website.
491 Favez, O., Sciare, J., Cachier, H., Alfaro, S. C., Abdelwahab, M. M., 2008. Significant formation
492 of water-insoluble secondary organic aerosols in semi- arid urban environment. Geophysical
493 Research Letters 35, L15801.
494 Grivas, G., Cheristanidis, S., Chaloulakou, A., 2012. Elemental and organic carbon in the urban
495 environment of athens. seasonal and diurnal variations and estimates of secondary organic
496 carbon. Science of the Total Environment 414(1), 535-545.
497 Guo, J. P., Miao, Y. C., Zhang, Y., Liu, H., Li, Z. Q., Zhang, W. C., He, J., Lou, M. Y., Yan, Y.,
498 Bian, L. G., Zhai, P. M., 2016. The climatology of planetary boundary layer height in China
499 derived from radiosonde and reanalysis data. Atmospheric Chemistry and Physics 16(20),
500 13309.
501 Han, S., Kondo, Y., Oshima, N., Takegawa, N., Miyazaki, Y., Hu, M., Lin, P., Deng, Z., Zhao, Y.,
502 Sugimoto, N., Wu, Y., 2009. Temporal variations of elemental carbon in Beijing. Journal of
503 Geophysical Research: Atmospheres 114(D23), DOI: 10.1029/2009JD012027.
504 He, K. B., Yang, F. M., Duan, F. K., Ma Y. L., 2011. Atmospheric Particulate Matter and Regional
505 Complex Pollution. Science Press, Beijing, China. 310-327.
506 He, K. B., Yang, F. M., Ma, Y. L., Zhang, Q., Yao, X. H., Chan, C. K., Cadle, S., Chan, T., Mulawa,

P., 2001. The characteristics of $PM_{2.5}$ in Beijing, China. Atmos. Environ. 35: 4959–4970.

Jeong, B., Bae, M. S., Ahn, J., Lee, J., 2017. A study of carbonaceous aerosols measurement in metropolitan area performed during korus-aq 2016 campaign. Journal of Korean Society for Atmospheric Environment, 33.

Ji, D. S., Li, L., Pang, B., Xue, P., Wang, L. L., Wu, Y. F., Zhang, H. L., Wang, Y. S., 2017. Characterization of black carbon in an urban-rural fringe area of Beijing. Environmental Pollution 223, 524-534.

Ji, D. S., Li, L., Wang, Y. S., Zhang, J. K., Cheng, M. T., Sun, Y., Liu, Z. R., Wang, L. L., Tang, G. Q., Hu, B., Chao, N., Wen, T. X., Miao, H. Y., 2014. The heaviest particulate air-pollution episodes occurred in northern China in January, 2013: Insights gained from observation. Atmospheric Environment 92, 546-556.

Ji, D. S., Zhang, J. K., He, J., Wang, X. J., Pang, B., Liu, Z. R., Wang, L. L., Wang, Y. S., 2016. Characteristics of atmospheric organic and elemental carbon aerosols in urban Beijing, China. Atmospheric Environment 125, 293-306.

Keuken, M. P., Jonkers, S., Zandveld, P., Voogt, M., 2012. Elemental carbon as an indicator for evaluating the impact of traffic measures on air quality and health. Atmospheric Environment 61, 1-8.

Kleinman, L. I., Springston, S. R., Daum, P. H., Lee, Y. N., Nunnermacker, L. J., Senum, G. I., Wang, J., Weinstein-Lloyd, J., Alexander, M. L., Hubbe, J., Ortega, J., Canagaratna, M. R., Jayne, J., 2008. The time evolution of aerosol composition over the Mexico City plateau. Atmospheric Chemistry and Physics 8, 1559-1575.

Lin, P., Hu, M., Deng Z, Slanina, J., Han, S., Kondo, Y., Takegawa, N., Miyazaki, Y., Zhao, Y.,

529 Sugimoto, N., 2009. Seasonal and diurnal variations of organic carbon in $PM_{2.5}$ in Beijing
530 and the estimation of secondary organic carbon. Journal of Geophysical Research:
531 Atmospheres 114(D2), DOI: 10.1029/2008JD010902.
532 Lu, Z., Zhang, Q., Streets, D. G., 2011. Sulfur dioxide and primary carbonaceous aerosol
533 emissions in China and India, 1996–2010. Atmospheric Chemistry and Physics 11,
534 9839-9864.
535 Mancilla, Y., Mendoza, A., 2012. A tunnel study to characterize $PM_{2.5}$ emissions from
536 gasoline-powered vehicles in Monterrey, Mexico. Atmospheric environment 59, 449-460.
537 Mauderly, J. L., Chow, J. C., 2008. Health effects of organic aerosols. Inhalation toxicology 20(3),
538 257-288.
539 Miao, L., Liao, X. N., Wang, Y. C., 2016. Diurnal Variation of $PM_{2.5}$ Mass Concentration in
540 Beijing and Influence of Meteorological Factors Based on Long Term Date. Environmental
541 Science, 37(8), 2836-2846.
542 Odum, J., Hoffmann, T., Bowman, F., Collins, R., Flagan, J., Seinfeld, J. H., 1996. Gas/particle
543 partitioning and secondary organic aerosol yields. Environmental Science and Technology 30,
544 2580-2585.
545 Pan, X. L., Kanaya, Y., Wang, Z. F., Liu, Y., Pochanart, P., Akimoto, H., Sun, Y. L., Dong, H. B.,
546 Li, J., Irie, H., Takigawa, M., 2011. Correlation of black carbon aerosol and carbon monoxide
547 in the high-altitude environment of Mt. Huang in Eastern China. Atmospheric Chemistry and
548 Physics 11, 9735-9747.
549 Pan, X. L., Kanaya, Y., Wang, Z. F., Taketani, F., Tanimoto, H., Irie, H., Takashima, H., Inomata,
550 S., 2012. Emission ratio of carbonaceous aerosols observed near crop residual burning
551 sources in a rural area of the Yangtze River Delta Region, China. Journal of Geophysical

552 Research: Atmospheres, 117(D22).
553 Pandis, S. N., Harley, R. A., Cass, G. R., 1992. Secondary organic aerosol formation and transport.
554 Atmospheric Environment Part A. General Topics 26(13), 2269-2282.
555 Polissar, A. V., Hopke, P. K., Paatero, P., Kaufmann, Y. J., Hall, D. K., Bodhaine, B. A., Dutton, E.
556 G., Harris, J. M., 1999. The aerosol at Barrow, Alaska: long-term trends and source locations.
557 Atmospheric Environment 33(16), 2441-2458.
558 Pope III, C. A., Dockery, D. W., 2006. Health effects of fine particulate air pollution: lines that
559 connect. Journal of the air & waste management association 56(6), 709-742.
560 Ren, Z. H., Wan, B. T., Yu, T., Su, F. Q., Zhang, Z. G., Gao, Q. X., Yang, X. X., Hu, H. L., Wu, Y.
561 H., Hu, F., Hong, Z. X., 2004. Influence of Weather System of Different Scales on Pollution
562 Boundary Layer and the Transport in Horizontal Current Field. Research of Environmental
563 Sciences 17(1), 7-13.
564 Schauer, J. J., Kleeman, M. J., Cass, G. R., Simoneit, B. R., 2001. Measurement of emissions from
565 air pollution sources. 3. C1-C29 organic compounds from fireplace combustion of wood.
566 Environmental Science & Technology 35(9), 1716-1728.
567 Schauer, J. J., Kleeman, M. J., Cass, G. R., Simoneit, B. R., 2002. Measurement of emissions from
568 air pollution sources. 5. C1− C32 organic compounds from gasoline-powered motor vehicles.
569 Environmental science & technology 36(6), 1169-1180.
570 Seinfeld, J. H., & Pandis, S. N. (2016). Atmospheric chemistry and physics: from air pollution to
571 climate change. John Wiley & Sons.
572 Seinfeld, J. H., Erdakos, G. B., Asher, W. E., Pankow, J. F., 2001. Modeling the Formation of
573 Secondary Organic Aerosol (SOA). 2. The Predicted Effects of Relative Humidity on Aerosol

574 Formation in the α-Pinene-, β-Pinene-, Sabinene-, Δ^3-Carene-, and Cyclohexene-Ozone
575 Systems. Environmental Science and Technology 35(9), 1806-1817.
576 Singer, B., Kirchstetter, T., Harley, R., Kendall, G., Hesson, J., 1999. A fuel based approach to
577 estimating motor vehicle cold-start emissions. Journal of the Air & Waste Management
578 Association 49(2), 125-135.
579 Sun, Y., Jiang, Q., Wang, Z., Fu, P., Li, J., Yang, T., Yin, Y., 2014. Investigation of the sources and
580 evolution processes of severe haze pollution in Beijing in January 2013. Journal of
581 Geophysical Research: Atmospheres 119(7), 4380-4398.
582 The Intergovernmental Panel on Climate Change (IPCC), Fifth Assessment Report (AR5) 2013.
583 http://www.ipcc.ch/report/ar5/wg1/
584 Wang, Y. Q., Zhang, X. Y., Draxler, R. R., 2009. TrajStat: GIS-based software that uses various
585 trajectory statistical analysis methods to identify potential sources from long-term air
586 pollution measurement data. Environmental Modelling & Software 24(8), 938-939.
587 World Health Organization, 2005. http://apps.who.int/iris/bitstream/10665/69477/1/WHO_SDE_
588 PHE_OEH_06.02_eng.pdf.
589 Wu, D., Liao, B. T., Wu, M., Chen, H. Z., Wang, Y. C., Liao, X. N., Gu, Y., Zhang, X. L., Zhao, X.
590 J., Quan, J. N., Liu, W. D., Meng, J. P., Sun, D., 2014. The long-term trend of haze and fog
591 days and the surface layer transport conditions under haze weather in North China. Acta
592 Scientiae Circumstantiae (in Chinese) 34(1), 1-11.
593 Yao, Q., Zhao, P. S., Han, S. Q., Liu, A. X., 2014. Pollution character of carbonaceous aerosol in
594 $PM_{2.5}$ in Tianjin City. Environmental Chemistry (in Chinese) 33, 404-410.
595 Zhao, P. S., Dong, F., Yang, Y. D., He, D., Zhao, X. J., Zhang, W. Z., Yao, Q., Liu, H. Y., 2013.

596 Characteristics of carbonaceous aerosol in the region of Beijing, Tianjin, and Hebei, China.
597 Atmospheric Environment 71, 389-398.
598 Zheng, G. J., Duan, F. K., Su, H., Ma, Y. L., Cheng, Y., Zheng, B., Zheng, B., Zhang, Q., Huang,
599 T., Kimoto, T., Chang, D., Pöschl, U., Cheng, Y. F., He, K. B., 2015. Exploring the severe
600 winter haze in Beijing: the impact of synoptic weather, regional transport and heterogeneous
601 reactions. Atmospheric Chemistry and Physics 15(6), 2969-2983.

Highlights (3 to 5 bullet points (maximum 85 characters including spaces per bullet point)

- The average OC and EC concentrations did not decline as expected.
- The mass fractions of OC and EC in $PM_{2.5}$ declined when the air quality deteriorated.
- No clear weekend effects were observed in contrast to developed regions.
- A much smaller source region was identified in the winter than in the other seasons.

*Revised manuscript with no changes marked
Click here to view linked References

Two-year continuous measurements of carbonaceous aerosols in urban Beijing, China: temporal variations, characteristics and source analyses

Dongsheng Ji[1*], Yingchao Yan[1, 2], Zhanshan Wang[3], Jun He[4], Baoxian Liu[3], Yang Sun[1], Meng Gao[5], Yi Li[6], Wan Cao[1, 2], Yang Cui[1, 2], Bo Hu[1], Jinyuan Xin[1], Lili Wang[1], Zirui Liu[1], Guiqian Tang[1], Yuesi Wang[1*]

[1] *State Key Laboratory of Atmospheric Boundary Layer Physics and Atmospheric Chemistry, Institute of Atmospheric Physics, Chinese Academy of Sciences, Beijing, China*

[2] *University of Chinese Academy of Sciences, Beijing, China*

[3] *Beijing Municipal Environmental Monitoring Center, Beijing, China*

[4] *Natural Resources and Environment Research Group, International Doctoral Innovation Centre, Department of Chemical and Environmental Engineering, University of Nottingham Ningbo China, Ningbo, China*

[5] *John A. Paulson School of Engineering and Applied Sciences, Harvard University, Cambridge MA, USA*

[6] *Arizona Department of Environmental Quality, Phoenix, AZ, USA*

* Corresponding author

Email address: jds@mail.iap.ac.cn; wys@dq.cern.ac.cn

Abstract

Organic carbon (OC) and elemental carbon (EC) in the $PM_{2.5}$ of urban Beijing were measured hourly with a semi-continuous thermal-optical analyzer from Jan 1, 2013 to Dec 31, 2014. The annual average OC and EC concentrations in Beijing were 17.0±12.4 and 3.4±2.0 $\mu g/m^3$ for 2013, and 16.8±14.5 and 3.5±2.9 $\mu g/m^3$ for 2014. It is obvious that the annual average concentrations of OC and EC in 2014 were not less than those in 2013 while the annual average $PM_{2.5}$ concentration (89.4 $\mu g/m^3$) in 2014 was slightly reduced as compared to that (96.9 $\mu g/m^3$) in 2013. Strong seasonality of the OC and EC concentrations were found with high values during the heating seasons and low values during the non-heating seasons. The diurnal cycles of OC and EC characterized by higher values at night and in the morning were caused by primary emissions, secondary transformation and stable meteorological condition. Due to increasing photochemical activity, the OC peaks were observed at approximately noon. No clear weekend effects were observed. Interestingly, in the early mornings on weekends in the autumn and winter, the OC and EC concentrations were close to or higher than those on weekdays. Our data also indicate that high OC and EC concentrations were closely associated with their potential source areas which were determined based on the potential source contribution function analysis. High potential source areas were identified and were mainly located in the south of Beijing and the plain of northern China. A much denser source region was recorded in the winter than in the other seasons, indicating that local and regional transport over regional scales are the most important. These results demonstrate that both regional transport from the southern regions and local accumulation could lead to the enhancements of OC and EC and likely contribute to the severe haze pollution in Beijing.

Keywords OC, EC, $PM_{2.5}$, Beijing, Meteorological effects

1. Introduction

Organic carbon (OC) and elemental carbon (EC) represent major fractions of $PM_{2.5}$ and play important roles in the states of human health, the atmospheric environment and climate change (Bond et al., 2013; World Health Organization, 2005; Seinfeld and Pandis, 2016; IPCC AR5, 2013). Epidemiologic studies illustrate the risks of exposure to these particles by showing that the increasing levels of OC and EC in urban areas were closely associated with cardiovascular mortality and morbidity (Pope et al., 2006; Mauderly et al., 2008). In addition, OC, which includes polycyclic aromatic hydrocarbons (PAHs) and polychlorinated biphenyls (PCBs), has the potential to induce carcinogenic and mutagenic effects, while EC, which includes mediums carrying heavy metals and PAHs, has adverse effects on public health (Biswas et al., 2009). In addition to health risks, OC, EC and the mixing of OC and EC with anthropogenic inorganic constituents have been shown to result in the degradation of air quality and visibility impairments (Ji et al., 2017). Furthermore, OC and EC have significant effects on the Earth radiation balance and, in turn, on the climate at both global and regional scales through direct and indirect radiative forcing. OC and EC also play key roles in the formation of cloud condensation nuclei, resulting in higher albedos of cloud and more intense monsoon circulation and rainfall patterns (Bond et al., 2013). Therefore, worldwide attention has been paid to studies of OC and EC. In particular, there is greater concern regarding the high emissions of OC and EC in rapidly developing countries.

High loadings of OC and EC have been recorded in China for decades (Lu et al., 2011; Pan et al., 2011, 2013). As one of the most developed agglomerations in China, the Beijing-Tianjin-Hebei (BTH) region is heavily influenced by anthropogenic emissions, resulting in severe air pollution

(Zhao et al., 2013). A series of field measurements of OC and EC were carried out in the North Plain of China, including in Beijing, Tianjin and Hebei province (Cheng et al., 2013; Ji et al., 2014, 2016; Andersson et al., 2015). As reported by Yao et al. (2014), spatial differences in the OC and EC occurrence levels were found in the BTH region, and high concentrations were observed in the autumn and winter. He et al. (2001) presented the concentrations of OC and EC in $PM_{2.5}$ and found that carbonaceous aerosols (CAs) are the main components of $PM_{2.5}$ in Beijing. Ji et al. (2016) concluded that clean energy strategies led to effective declines in the OC and EC concentrations, and high concentrations of secondary organic carbon (SOC) were observed in the autumn and winter. The previous studies of OC and EC were mainly based on filter sampling for multiple hours or several days and on subsequent laboratory analyses, all of which are susceptible to sampling and analysis artifacts (uncertainty of the artificial sampling was relative larger.) (Cheng et al., 2011). Additionally, the low temporal-resolved results can mask detailed variations and characteristics of OC and EC. Yearly high-temporal-resolution studies of OC and EC are invariably scarce (Lin et al., 2009; Zhao et al., 2013; Ji et al., 2016; Chang et al., 2017). It is therefore necessary to study the variation, accumulation and transport of OC and EC as well as the relationship between OC and EC to understand the processes and sources affecting the evolution of OC and EC based on high-time resolved continuous in situ measurements.

Most of previous studies were conducted before the implementation of the Air Pollution Prevention and Control Action Plan in September 2013. After the execution of this action plan, air quality improved in Beijing, with the annual mean $PM_{2.5}$ concentrations declining from 96.9 in 2012 to 89.4 $\mu g/m^3$ in 2013. Although a decline in the $PM_{2.5}$ concentrations was observed, the annual mean $PM_{2.5}$ concentrations were still much higher than the secondary Chinese annual mean

89 $PM_{2.5}$ standard (35 μg/m^3) and the World Health Organization's annual-average guideline for
90 $PM_{2.5}$ (15 μg/m^3). Considering that OC and EC account for high fractions of $PM_{2.5}$ (He et al., 2001,
91 2011; Cao et al., 2004) and are closely associated with fuel combustion, thus, scientific knowledge
92 of OC and EC is a prerequisite for effectively establishing and enforcing preventative and
93 corrective measures concerning fossil fuel consumption-related emissions as well as for finally
94 attaining both national and international $PM_{2.5}$ standards. However, the effectiveness of emission
95 abatement and pollution control measures on ambient OC and EC have seldom been analyzed in
96 Beijing in detail.

97 In the present study, two-year hourly OC and EC concentrations were observed using a
98 semi-continuous OC/EC analyzer in the central zone of Beijing from Jan 1, 2013, to Dec 31, 2014.
99 To the best of our knowledge, this was the comprehensive study of OC and EC in the urban core
100 area of Beijing based on continuous two-year-long hourly time-resolved OC, EC, $PM_{2.5}$ and
101 meteorological parameter data. This work was part of the campaign sponsored by the Strategic
102 Priority Research Program of the Formation, Mechanism and Control Strategies of Haze in China,
103 launched by the Chinese Academy of Sciences (CAS). One of the purposes of this program was to
104 better understand the characteristics of the chemical compositions of $PM_{2.5}$ in China and to
105 evaluate the efficiencies of air pollution control measures for air quality improvement. In addition,
106 the strictest air pollution control measures were implemented during the study period, and a
107 comparative analysis was carried out between the pre- and post-implementation states of these
108 measures as energy structure and policy were expected to change significantly. The OC and EC
109 characteristics and their seasonal and diurnal variations are discussed. Finally, the potential source
110 areas contributing to the high concentrations of OC and EC during the four seasons are analyzed

111 using potential source contribution function (PSCF) analysis.

112 **2. Experiments**

113 **2.1 Measurement site**

114 As shown in Fig. 1, the sampling point (39°55′38″ N, 116°19′29″ E, 40 m Alt) surrounded by
115 residential areas and without any nearby industrial source is a typical urban site in the central zone
116 of Beijing. It is located approximately 1.2 km away from the west 3rd Ring Road and 2.7 km
117 away from the north 2nd Ring Road. Both ring roads are characterized by heavy traffic
118 (http://www.bjtrc.org.cn/JGJS.aspx?id=5.2&Menu=GZCG), and their annual-average vehicular
119 speeds during the morning (7:00-9:00) and evening traffic peaks (17:00-19:00) were 27.4 and 24.2
120 km/h and 27.8 and 23.2 km/h in 2013 and 2014, respectively. The sampling campaign was
121 conducted from January 1, 2013 to December 31, 2014.

122 As shown in Fig. S1(a), obvious seasonal distributions were recorded for the atmospheric
123 temperature (*T*), relative humidity (*RH*), wind speed (*WS*) and direction (*WD*), atmospheric
124 pressure (*P*), UV radiation (*UV*), precipitation (*Prec.*) and mixed layer height (MLH). The
125 monthly average RH was higher than 50 % in the summer and reached its minimum value
126 (approximately 30 %) in the spring. *T* and *UV* showed similar seasonal cycles characterized by
127 low values in the winter and high values in the summer. The monthly variations of WS varied
128 from 1.0 to 2.0 m/s, with slightly higher values in the spring. In addition, the rainy season lasted
129 from June to September, while precipitation was almost negligible during the wintertime.

130 **2.2 Instrumentation**

131 Hourly OC and EC concentrations of $PM_{2.5}$ were recorded using a OC/EC analyzer (Model 4,
132 Sunset Laboratory Inc. Oregon, USA) with the thermal-optical transmission method. Volatile

133 organic compounds were removed by inline parallel carbon denuder removing installed on the
134 analyzer. Round 16-mm quartz filters were used for collecting OC and EC samples at a sampling
135 flow rate of 8 L/min. OC and EC samples were collected for 40 minutes and then were analyzed in
136 approximately 15 minutes. The multiple programmed steps were based on the NIOSH 5040
137 thermal protocol, which has been introduced by Cassinelli et al. (1998). A non-dispersive infrared
138 (NDIR) detector was used for quantifying particulate OC and EC concentrations. For the charring
139 correction, the sample transmittance was recorded by a He-Ne laser beam (665 nm wavelength)
140 system throughout the analysis process. The split point between OC and EC was obtained when
141 the transmittance of laser signal returned to its initial value (Birch et al., 1996). The standard
142 procedure for calibration has been introduced in manual of the OC and EC analyzer in details
143 (https://www3.epa.gov/ttnamti1/files/ambient/pm25/spec/Sunset_Manual.pdf). The quartz fiber
144 filters used for sampling was changed when the laser correction factor drops below 0.90. An
145 instrument blank was conducted when the quartz fiber filters was changed. An internal standard
146 CH_4 mixture (5.0 %; ultrahigh purity He balance) was used to calibrate the analyzer automatically
147 at the end of every analysis. In addition, an off-line calibration was performed using an external
148 source of sucrose standard (2.06 g/L) every three months. The range of total carbon (TC, a sum of
149 OC and EC) for the NIOSH protocol varies from 0.7 to 70 μg C/cm^2 and the limit of detection
150 (LOD) is calculated at 0.15 μg C/cm^2 (Birch and Cary, 1996; Peterson and Richards, 2002). It
151 might be negligible for $PM_{2.5}$ to overestimate OC or EC caused by CC interference due to the
152 contribution of CC in $PM_{2.5}$ less than 5 % of TC.

153 Ambient $PM_{2.5}$, O_3, SO_2 and NO_2 were measured using a tapered element oscillating
154 microbalance $PM_{2.5}$ monitor with a Filter Dynamics Measurement System (Model 1405,

Thermo-Fisher Scientific (TE)), a UV photometric O_3 analyzer (Model 49i, TE), a pulsed fluorescence SO_2 analyzer (Model 43i, TE) and a chemiluminescence NO-NO_2-NO_x analyzer (Model 42i, TE), respectively. Detailed information on the ambient $PM_{2.5}$, O_3, SO_2 and NO_2 analyzers has been reported by Ji et al. (2014). The SO_2 and NO_2 analyzers were calibrated using a 50 ppmv SO_2 standard gas and a 52 ppmv NO standard gas (Scott-Marrin gases, Riverside, CA, USA), respectively. In addition, an O_3 calibrator (49I PS, TE), which can be traceable to the standard reference photometer at the US National Institute of Standards and Technology, was used to calibrate the O_3 analyzer. The CO concentrations at the Dingling station (issued by website, http://zx.bjmemc.com.cn/getAqiList.shtml?timestamp=1507517944788) were selected as the $CO_{background}$ concentrations.

Hourly data of atmospheric temperature (*T*), relative humidity (*RH*), ultraviolet radiation (*UV*), wind speed (*WS*) and direction (*WD*), precipitation (*Prec.*) and mixed layer height (MLH), were downloaded from the meteorological tower of the Institute of Atmospheric Physics (IAP), CAS during the sampling periods.

2.3 PSCF analysis

Potential source contribution function (PSCF) analysis can be used to identify possible source areas affecting air pollution levels. In principle, PSCF uses backward trajectories to determine potential locations of emission sources. The PSCF is defined as:

$$\mathrm{PSCF}(i,j) = W_{ij} \times (m_{ij}/n_{ij}) \quad (1)$$

where n_{ij} is the total number of back-trajectory segment endpoints that fall into the grid cell (i, j), n_{ij} is the number of points with concentrations of air pollutants higher than a threshold value (m_{ij}) and W_{ij} is an empirical weight function proposed to reduce the uncertainty of n_{ij} during the study

period. Higher ratios of m_{ij}/n_{ij} illustrate higher probability of particular grids through which passing air masses will lead to higher receptor concentrations.

The National Oceanic and Atmospheric Administration Hybrid Single-Particle Lagrangian Integrated Trajectory model (HYSPLIT 4.9) were used for calculating the 48 h backward trajectories terminating at the study site at a height of 100 m every 1 hour during the sampling period (Draxler and Rolph, 2003). In this study, the domain for the PSCF was set in the range of (30-60 °N, 65-150 °E). The 75th percentile for OC and EC for each season was used as the threshold values to calculate m_{ij}. A weighting function (w_{ij}) introduced by Wang et al. (2009) and Polissar et al. (1999) was used in the PSCF to reduce the uncertainties for those grid cells with a limited number of points in each season of 2013 and 2014.

3. Results and discussion

3.1 Occurrence levels of OC and EC

The distributions of OC and EC at the urban sampling site in Beijing from 2013 to 2014 are presented in Fig. 2. As shown in Fig. 2, the hourly OC concentrations ranged from 1.1 to 143.1 μg/m^3 and from 0.3 to 135.1 μg/m^3 with averages of 17.0 ± 12.4 μg/m^3 and 16.8 ± 14.5 μg/m^3 in 2013 and 2014, respectively. In addition, the EC concentrations ranged from 0.2 to 28.1 and from 0.2 to 31.7 μg/m^3 with averages of 3.4 ± 2.0 μg/m^3 and 3.5 ± 2.9 μg/m^3, respectively. The average OC concentration was higher than that (14.5±12.1 μg/m^3) observed at the IAP site located between the north 3rd Ring and 4th Ring roads in urban Beijing (shown in Fig. 1), while the average EC concentration was lower than that (4.4±4.0 μg/m^3) observed at the IAP site. In contrast to the results observed at the IAP site, the OC/EC ratios were 6.6±4.5 and 6.5±3.2 in 2013 and 2014, respectively, which were higher, suggesting the spatial differences in the emissions of

OC and EC in urban Beijing.

The contributions of OC and EC to the measured $PM_{2.5}$ mass concentrations were averagely 17.6 and 3.5 %, respectively, in 2013 and 18.8 and 4.0 % in 2014. OC accounted for 83.3 ± 8.5 and 82.6±7.4 % of the TC for these two years, indicating that OC was the predominant carbon contributor. In this study, the contributions of TC to $PM_{2.5}$ were found to be 21.1 ± 19.1 and 22.7 ± 29.9 % in 2013 and 2014, respectively, which were similar with those reported in Beijing's 2012 Environmental Status (e.g., the contributions of TC to $PM_{2.5}$ accounted for approximately 21.6 %). The carbonaceous aerosol levels were estimated as the sum of the OC multiplied by 1.4 and the EC concentrations, which accounted for 28.0 ± 26.7 and 30.2 ± 41.9 % of the recorded $PM_{2.5}$ values in 2013 and 2014, respectively, suggesting that the carbonaceous fraction could contribute significantly to the fine particles. The variations of the concentrations and ratios of OC and EC varying with the incremental $PM_{2.5}$ concentrations were also discussed. As shown in Figs. S2(a) and S2(b), Beijing experienced different air quality days classified based on the daily $PM_{2.5}$ concentrations in 2013 and 2014, which were defined as excellent ($0<PM_{2.5}\leq35$ μg/m^3), good ($35<PM_{2.5}\leq75$ μg/m^3), lightly polluted (LP, $75<PM_{2.5}\leq115$ μg/m^3), moderately polluted (MP, $115<PM_{2.5}\leq150$ μg/m^3), heavily polluted (HP, $150<PM_{2.5}\leq250$ μg/m^3) and severely polluted (SP, $PM_{2.5}>250$ μg/m^3), respectively. Approximately 50 % of the days were classified as polluted days (days with daily average $PM_{2.5}$ concentrations greater than 75 μg/m^3) in 2013 and 2014 in Beijing. The OC and EC concentrations were significantly enhanced with the increase of $PM_{2.5}$ concentrations. Note that the OC/EC ratios in 2014 declined significantly when air quality became heavily and severely polluted days in contrast to those in 2013. As reported by Schauer et al. (2001, 2002), the OC/EC ratio could suggest the sources of aerosol particles, and such a ratio of

aerosols emitted from coal combustion was higher than that from vehicles. During heavily polluted and severely polluted days, local emissions played dominant roles in the accumulation of aerosol particles because air masses were stagnant (Sun et al., 2014). The significant decrease of the OC/EC ratios could imply that coal combustion might have been banned to a greater extent after the enforcement of the new air pollution control action plan in 2014, while vehicular emission appeared to be more pronounced during heavily and severely polluted days.

3.2 Seasonal characteristics of OC and EC

Fig. 2 depicts the seasonal variations in OC and EC during the study periods. The observed OC concentrations exhibited strong seasonality in both 2013 and 2014. Higher concentrations were found in the heating seasons (from Nov 15 to Mar 15) while lower concentrations were found in the non-heating seasons in Beijing. The average OC concentrations were 23.0 ± 17.6 and 24.5 ± 20.2 $\mu g/m^3$ in the heating seasons of 2013 and 2014, respectively, while the OC concentrations were 14.0 ± 7.0 and 13.1 ± 8.3 $\mu g/m^3$ in the non-heating seasons of 2013 and 2014, respectively. The extra fossil fuel consumed for heating clearly led to higher emissions of OC during the heating seasons. In addition, the higher OC concentrations observed may also be attributed to secondary formations of increased amounts of OC precursors from extra fuel combustion used for heating through condensation processes during the unfavorable meteorological conditions like low temperatures and wind speed as well as high humidity in the winter (Pandis et al. 1992; Odum et al. 1996). The low temperature is favorable for semi-volatile OC condensed onto existing particles and high RH being conducive to the dissolution of water-soluble gases into liquid aerosol particles are known to result in further chemical reactions within these particles, which contributes to the OC concentrations (Seinfeld and Pandis, 2016).

Additionally, cold starts of vehicles result in significantly higher emissions of carbonaceous particles and their precursors in the winter (Singer et al., 1999). Conversely, high atmospheric temperature result in more VOCs partitioned into the gas phase (Pandis et al., 1992; Odum et al., 1996). In contrast to heating seasons, less fossil fuel is consumed for heating in the non-heating seasons, and the lower OC concentrations were observed in the spring, the summer and most of the autumn. Besides residential heating, other energy consumed by transport and industry was also important OC sources, but these sources almost have no seasonal differences except for in the winter.

In addition to the contributions of sources, different weather conditions also play important roles in the seasonal differences of OC concentrations. In the autumn, the average wind speeds were 1.1 and 1.0 m/s in 2013 and 2014, respectively, which were the lowest of the four seasons. The average pressures were 1,013.4 and 1,013.0 hPa in these two years, respectively, and uniform pressure systems frequently dominated northern China in the autumn. Due to the weak pressure gradient, the meteorological conditions were conducive to air pollutant accumulations, thus, led to high OC concentrations. The highest WS recorded in the spring was conducive to air pollutant dispersion and transport, while the frequent precipitation could remove more air pollutants in the summer. These meteorological conditions resulted in lower OC concentrations in the spring and summer. In addition, the lowest OC concentration observed in the summer was also because high ambient temperatures will help shift the gas-particle partitioning of semi-volatile organic compounds toward the gaseous phase. The differences in OC values between the winter and summer could suggest seasonal variations in emission sources (Zhao et al., 2013). The ratios of OC_{spring}/OC_{summer}, OC_{autumn}/OC_{summer} and OC_{winter}/OC_{summer} were 1.0, 0.8 and 1.6 for 2013 and 1.2,

1.6 and 2.1 for 2014, respectively. To exclude the dispersion effect of the planetary boundary layer (PBL), the ratios of OC/ΔC_{CO} (C_{co}-$C_{co\ background}$, Kleinman et al., 2008) can be widely used for the analyses in this study. The ratio of OC/ΔC_{CO} shows similar seasonal variation with OC concentrations. The ratios of OC/ΔC_{CO} between the winter and summer were 1.07 for 2013 and 1.06 for 2014, respectively, suggesting that fossil fuel used for heating plays an important role in the OC concentrations in urban Beijing and that more efforts to control residential heating emissions are needed to improve air quality in Beijing.

The average EC concentrations in the winter were approximately 1.5 and 2.1 times higher than those in the summers of 2013 and 2014, respectively. Note that the differences in the EC concentrations between the winter and summer were higher than those observed in the north and northwest of the urban center of Beijing before the 2008 Olympic Games (Han et al., 2009). By comparison, effective control of coal consumption and highly polluting vehicles played important roles in the decline in EC concentrations. Moreover, the EC concentrations obviously declined more significantly in the summer than in the winter. As shown in the Beijing statistics yearbook, natural gases and electrical appliance were widely used to replace coal and heavily polluting motorized vehicles were banned (http://www.bjstats.gov.cn/nj/main/2015-tjnj/indexch.htm). In addition, household honeycomb-briquette burning and small stoves for cooking and heating were strictly banned inside the 4th ring of Beijing. This was consistent with the decline in the volume of coal consumption.

Similar to OC, higher EC concentrations in $PM_{2.5}$ were observed in the autumn and winter, while lower levels were recorded in the spring and summer. The highest EC concentrations in $PM_{2.5}$ were recorded in the winter with averages of 4.1±2.2 and 4.9±3.9 μg/m^3 for 2013 and 2014,

287 respectively, which were lower than the previous results observed in the autumn (Hu et al., 2009;
288 Zhao et al., 2013). These observations suggest that improvement of air quality in Beijing through
289 governmental and public efforts were effective in somewhat reducing EC concentrations despite
290 the rapidly multiplying vehicle fleet within the municipality. The average concentrations of EC in
291 the autumn of 2013 and 2014 were approximately 1.3 and 1.9 times higher than those in the
292 summers. Lower occurrence levels of EC (with averages of 2.7 ± 1.7 and 2.1 ± 1.2 μg/m^3 for 2013
293 and 2014, respectively) in the summer could be attributed to favorable meteorological conditions
294 (e.g., strong and frequent precipitation and high MLH height) and low emission intensities.

295 **3.3 Diurnal characteristics of OC and EC**

296 As shown in Fig. 3 (a), the obvious diurnal OC and EC variations were observed in the four
297 seasons in 2013 and 2014. The EC peaks were associated with rush hours, indicating that
298 vehicular emission resulted in these spikes. The EC concentrations remained at high levels from
299 the nighttime to early the next morning, likely due to stable meteorological conditions caused by
300 the decay of PBL (Miao et al., 2016; Guo et al., 2016) and the emissions from both heavy-duty
301 diesel trucks (HDDT) and heavy-duty vehicles (HDV). That is because that HDV and HDDT are
302 allowed to enter urban areas inside the 5th Ring Road from 0:00 to 06:00 (Local Time) by Beijing
303 Traffic Management Bureau (http://www.bjjtgl.gov.cn/Inquiries/roadControl.asp), whereas, at
304 other times, both higher PBL heights and lower EC emission intensities from HDV and HDDT
305 occurred. It was obvious that in the winter large-amplitude variations in the average EC
306 concentrations were recorded. The maximum peak concentrations (0:00-10:00) were 1.4, 1.5, 1.6
307 and 1.8 times higher than those observed in the valley concentrations (13:00-15:00) for the spring,
308 summer, autumn and winter, respectively.

309 The peak diurnal OC patterns were associated with traffic conditions in the four seasons of
310 2013 and 2014. In addition, one small additional peak occurred between 12:00 and 14:00, likely
311 due to the SOC formation caused by increases in solar radiation during midday. Note that the OC
312 peaks occurred from evening traffic rush hour to early the next morning, which can also be caused
313 by the decay of PBL and stronger traffic emissions as discussed for the above EC peak patterns.
314 Note that it was obvious that OC and EC concentrations in the autumn and winter of 2014
315 were higher than or close to those in 2013 while OC and EC concentrations in the spring and
316 summer of 2014 were higher than those in 2013 based on diurnal variations of OC and EC
317 concentrations. The results were similar with the variation of $PM_{2.5}$, showing that the frequent
318 occurrence of severe pollution episode in the autumn and winter was closely associated with the
319 roaring increase in $PM_{2.5}$ concentrations although evident improvement in air quality was
320 observed in the spring and summer. The synergetic effect of high emission, unfavorable
321 meteorological condition and regional transport in the autumn and summer offsetting the air
322 quality betterment in the other two seasons led to no marked decline in annual average
323 concentrations of OC and EC.
324 **3.4 Weekend effects**
325 The weekly cycles of OC and EC are of great interest because they provide insights into how
326 these pollutants respond to changes in anthropogenic emissions on weekdays and weekends. As
327 shown in Fig. 3(b), the diurnal cycles of OC and EC on weekdays and weekends were recorded
328 for 2013 and 2014. Differing from previous studies (Grivas et al., 2012; Jeong et al., 2017), no
329 clear weekend effects were observed. The average OC and EC concentrations on the weekends
330 were 17.5±13.9 and 3.4±2.0 μg/m^3 for 2013 and 16.7±12.0 and 3.6±2.7 μg/m^3 for 2014,

331 respectively, while those on the weekdays were 16.8±11.8 and 3.4±2.0 μg/m^3 for 2013 and 16.5
332 ±12.5 and 3.5±3.0 μg/m^3 for 2014, respectively. The average OC and EC concentrations during
333 the weekdays were lower or close to those during the weekends in 2013 and 2014, respectively. In
334 particular, the OC and EC concentrations in the early morning on weekends in the autumn and
335 winter were higher than those on weekdays. This suggests that there is no significant decline in
336 anthropogenic activity in the early mornings from weekdays to weekends. Conversely, enhanced
337 anthropogenic emissions might have occurred in the early mornings on weekends in the autumn
338 and winter. As mentioned above, HDV and HDDT are allowed to operate from 0:00 to 6:00 LT.
339 The enhancement of the OC and EC concentrations could be attributed to enhanced traffic
340 emissions, which are consistent with higher NO_x and CO concentrations (not shown). The above
341 results imply that more strict control of the emissions from HDV and HDDT should be carried out
342 on weekends.

343 **3.5 Source analysis**

344 Fig. 4 shows the relationships between the concentrations of OC and EC and the wind sectors
345 in the different seasons of 2013 and 2014. Higher concentrations of OC and EC frequently
346 occurred when the east (E), northwest (NW) and southerly winds prevailed in the spring and
347 summer, while lower concentrations occurred when the north (N) and northeast (NE) winds
348 prevailed. In the spring, the average OC and EC concentrations from the S were 16.4±6.3 and 3.1
349 ±1.3 μg/m^3 for 2013 and 12.9±6.2 and 2.5±1.3 μg/m^3 for 2014, respectively, which were
350 approximately 1.1 and 1.3 times and 1.2 and 1.1 times higher than those from the N for 2013 and
351 2014. However, the OC and EC gradients associated with the different wind sectors in the summer
352 were obviously lower than those in the spring. In the summer, the average OC and EC

353 concentrations from the SE were 15.5±5.7 and 2.7±2.5 μg/m^3 for 2013 and 13.3±4.6 and 2.2±
354 1.3 μg/m^3 for 2014. Higher OC and EC concentrations occurred more frequently as the wind
355 sectors changed along the N–NE–E–SE-S gradient, and then decreased along the S–SW–W-NW
356 gradient. Such a relationship between the wind sectors and the OC and EC concentrations is
357 remarkably consistent with the spatial distributions of $PM_{2.5}$ in northern China in 2013 and 2014
358 (China Environmental Statement, 2013, 2014). These results suggest that differences existed in the
359 air pollution around the study site in the autumn and winter. In fact, the average OC and EC
360 concentrations from the S were 13.3±5.7 and 2.8±1.7 μg/m^3 in the autumn of 2013 and were
361 15.7±4.6 and 3.2±2.6 μg/m^3 in the autumn of 2014, respectively. The winter season showed that
362 the OC and EC concentrations from the southerly wind ranged from 1.8 to 143.1 and 0.2 to 28.1
363 μg/m^3 in 2013 and 0.5 to 135.1 and 0.2 to 31.7 μg/m^3 in 2014, respectively, with OC being the
364 major fraction in $PM_{2.5}$, accounting for an average of 18.0 %.

365 Moreover, higher OC and EC concentrations were recorded when calm wind prevailed (Fig.
366 S1(b)). The relatively high OC and EC concentrations corresponded with southerly wind whereas
367 northerly winds with high speeds were favorable for low OC and EC concentrations. Thus, both
368 the long-range transport and local emissions played important roles in the OC and EC
369 concentrations.

370 A clear visualization of the extent of the regional transport and local emissions can be
371 obtained based on the PSCF results of the hourly resolved input data. As shown in Fig. 5, the
372 potential source areas for OC and EC varied among the four seasons of 2013 and 2014. There
373 were almost no differences in the potential source regions of OC and EC for 2013 and 2014, but
374 slight seasonal differences existed in the potential source regions of OC and EC. In the springs of

2013 and 2014, an obvious high potential source area of OC and EC was observed, located in the southern plain areas of Beijing, including parts of the Hebei, Shandong and Henan provinces. This pattern indicated that anthropogenic emissions from the southern plain areas of Beijing played important roles in the OC and EC concentrations in Beijing because the southern plain areas were heavily polluted areas influenced by high pollutant emissions from rapid economic growth, enhancements in energy consumption and vehicle population growth as well as industrial production.

In contrast to the contributions from the source regions in the spring, OC and EC had slightly smaller potential source regions in the summers of 2013 and 2014, the high potential source areas of OC and EC (>0.4) were also located to the south, southwest, and southeast of Beijing including Tianjin, Hebei and Shandong provinces. The PSCF plots of OC showed slightly different patterns to those of EC, potentially indicating a greater formation of secondary OC from volatile organic compounds from the source regions under high O_x conditions during the transport processes in the summer.

The potential source areas for OC and EC in the autumns of 2013 and 2014 were also similar to those in the spring. A distinct source area to the southeast of Beijing including Tianjin and the Bohai Sea, was also observed. The topography of the North China Plain agreed well with this pollution band, with the Taihang Mountains to the east and the Yan Mountains to the south, in particular for the adjacent areas of the Hebei and Shandong provinces. These results illustrate that regional transport from the south was involved in the formation of the severe air pollution in the autumn.

Large difference in PSCF distributions existed between winter and the other seasons. The high PSCF values were mainly located in the regions including the Hebei province, Tianjin, small parts of the Shanxi province, the Shandong province and Inner Mongolia. This pattern indicates that the cities far from Beijing are likely not very important sources of the wintertime CAs in Beijing. That is likely because stagnant synoptic conditions like low WS and temperature inversions occurred more frequently in the winter. Thus, local emissions and circulation from nearby or surrounding regions would have vital impacts on the pollution levels in Beijing. This result is consistent with those of previous studies, indicating that the transport of OC and EC from the SW to the NE along the Taihang Mountains in North Plain of China has been observed (Wu et al., 2014; Ren et al. 2004). Given that many highly polluted cities were located in this pathway, such as Shijiazhuang (annual average $PM_{2.5}$ value in 2014, 126 μg/m^3), Baoding (annual average $PM_{2.5}$ value in 2014, 129 μg/m^3) and Hengshui (annual average $PM_{2.5}$ value in 2014, 108 μg/m^3), regional transport from these regions would have a potentially high effect on the contributions of OC and EC in Beijing.

4. Conclusions

To understand the characteristics of $PM_{2.5}$-associated OC and EC in urban Beijing and to evaluate the effects of air pollution control measures on air quality improvement, two years of hourly OC and EC concentrations were recorded using a semi-continuous OC/EC instrument in the central zone of Beijing from Jan. 1, 2013 to Dec. 31, 2014. The following conclusions were obtained.

The average OC and EC concentrations were similar in 2013 and 2014. The mass fractions of OC and EC in $PM_{2.5}$ declined when the air quality deteriorated, indicating that inorganic aerosols

might have played more dominant roles in the formation of air pollution in Beijing during this study.

OC and EC showed distinctive seasonal and diurnal variations. The higher concentrations in the winter than those in the summer were largely because of enhanced coal combustion emissions. No clear weekend effects were observed in contrast to developed regions with clear weekly variations, possibly indicating stronger primary emissions in the atmosphere over Beijing. The significant decrease of the OC/EC ratios could imply that vehicular emission appeared to be more pronounced instead of coal combustion during heavily and severely polluted days.

Higher OC and EC concentrations were commonly related with wind from the S, E, and SE. A common high potential source area appeared to focus on the south of Beijing, along the Taihang Mountains in spring, summer and autumn, indicating the potentially high influence of the regional transport on OC and EC concentrations in Beijing. A much smaller source region was identified in the winter than in the other seasons, implying that the accumulations of local emissions and regional transport over smaller regional scales could contribute more significantly to the high air pollution events in the winter. The PSCF analysis clearly showed that stricter controls are needed for further mitigation of air pollution on a regional scale.

Acknowledgment

This work was supported by the National Key Research and Development Program of China (2016YFC0202701) and the Beijing Municipal Science and Technology Project (D17110900150000). The authors would like to thank all of the members of the LAPC/CERN in IAP, CAS, for maintaining the instruments used herein. We would also like to thank NOAA for providing the HYSPLIT and TrajStat model.

Reference

Andersson, A., Deng, J., Du, K., Zheng, M., Yan, C., Sköld. M., Gustafsson, Ö., 2015. Regionally varying combustion sources of the January 2013 severe haze events over eastern china. Environmental Science and Technology 49(4), 2038-2043.

Birch, M., Cary, R., 1996. Elemental carbon-based method for monitoring occupational exposures to particulate diesel exhaust. Aerosol Science & Technology 25(3), 221-241.

Peterson, M. R., Richards, M. H., 2002. Thermal-Optical-Transmittance Analysis for Organic, Elemental, Carbonate, Total Carbon, and OCX2 in $PM_{2.5}$ by the EPA/NIOSH Method. Research Triangle Institute.

Biswas, S., Verma, V., Schauer, J. J., Cassee, F. R., Cho, A. K., Sioutas, C., 2009. Oxidative potential of semi-volatile and non-volatile particulate matter (PM) from heavy-duty vehicles retrofitted with emission control technologies. Environmental Science & Technology 43(10), 3905-3912.

Bond, T. C., Doherty, S. J. Fahey, D. W., Forster, P. M., Berntsen, T., DeAngelo, B. J., Flanner, M. G., Ghan, S., Kärcher, B., Koch, D., Kinne, S., Kondo, Y., Quinn, P. K., Sarofim, M. C., Schultz, M. G., Schulz, M., Venkataraman, C., Zhang, H., Zhang, S., Bellouin, N., Guttikunda, S. K., Hopke, P. K., Jacobson, M. Z., Kaiser, J. W., Klimont, Z., Lohmann, U., Schwarz, J. P., Shindell, D., Storelvmo, T., Warren, S. G., Zender, C. S., 2013. Bounding the role of black carbon in the climate system: A scientific assessment. Journal of Geophysical Research: Atmospheres 118(11), 5380-5552.

Boparai, P., J. Lee, and T. C. Bond, 2008.Revisiting thermal-optical analyses of carbonaceous aerosol using a physical model. Aerosol Science and Technology 42, 930-948.

462 Cao, J., Lee, S., Ho, K., 2003. Characteristics of Carbonaceous Aerosol in Pearl River Delta
463 Region, China during 2001 Winter Period. Atmospheric Environment 37, 1451-1460.
464 Cao, J., Lee, S., Ho, K., 2004. Spatial and seasonal variations of atmospheric organic carbon and
465 elemental carbon in Pearl River Delta Region, China. Atmospheric Environment 38(27),
466 4447-4456.
467 Chang, Y. H., Deng, C. R., Cao, F., Cao, C., Zou, Z., Liu, S. D., Lee, X. H., Li, J., Zhang, G.,
468 Zhang, Y., 2017. Assessment of carbonaceous aerosols in Shanghai, China–Part 1: long-term
469 evolution, seasonal variations, and meteorological effects. Atmospheric Chemistry and
470 Physics 17(16), 9945-9964.
471 Cassinelli, M. E., O'Connor, P. F., 1998. NIOSH Method 5040. NIOSH Manual of Analytical
472 Methods (NMAM), Second Supplement to NMAM. 4th ed. DHHS (NIOSH) Publication,
473 94-113.
474 China Environmental Statement, 2013. http://www.mep.gov.cn/hjzl/zghjzkgb/lnzghjzkgb/201605/
475 P020160526564730573906.pdf
476 China Environmental Statement, 2014. http://www.mep.gov.cn/hjzl/zghjzkgb/lnzghjzkgb/201605/
477 P020160526564151497131.pdf
478 Cheng Y., 2011. Study on the Sampling and Analysis Methods of Carbonaceous Aerosol.
479 http://kns.cnki.net/KCMS/detail/detail.aspx?dbcode=CDFD&dbname=CDFD1214&filename
480 =1012035910.nh&v=MDQ1NzJyNUViUElSOGVYMUx1eFlTN0RoMVQzcVRyV00xRnJD
481 VVJMMmVadWR0RnlqbFc3M01WRjI2SExPN0c5ak4=
482 Cheng, Y., Engling, G., He, K. B., Duan, F. K., Ma, Y. L., Du, Z. Y., Liu, J. M., Zheng, M., Weber,
483 R. J., 2013. Biomass burning contribution to Beijing aerosol. Atmospheric Chemistry and

484 Physics 13, 7765–7781.

485 Chow, J., Watson, J., Pritchett, L., Pierson, W., Frazier, C., Purcell, P., 1993. The DRI
486 thermal/optical reflectance carbon analysis system: Description, evaluation and applications
487 in US air quality studies. Atmospheric Environment Part A 27(8), 1185-1201.

488 Draxler, R. R., & Rolph, G. D., 2003. HYSPLIT (HYbrid Single-Particle Lagrangian Integrated
489 Trajectory). NOAA Air Resources Laboratory, Silver Spring, MD. Model access via NOAA
490 ARL READY Website.

491 Favez, O., Sciare, J., Cachier, H., Alfaro, S. C., Abdelwahab, M. M., 2008. Significant formation
492 of water-insoluble secondary organic aerosols in semi- arid urban environment. Geophysical
493 Research Letters 35, L15801.

494 Grivas, G., Cheristanidis, S., Chaloulakou, A., 2012. Elemental and organic carbon in the urban
495 environment of athens. seasonal and diurnal variations and estimates of secondary organic
496 carbon. Science of the Total Environment 414(1), 535-545.

497 Guo, J. P., Miao, Y. C., Zhang, Y., Liu, H., Li, Z. Q., Zhang, W. C., He, J., Lou, M. Y., Yan, Y.,
498 Bian, L. G., Zhai, P. M., 2016. The climatology of planetary boundary layer height in China
499 derived from radiosonde and reanalysis data. Atmospheric Chemistry and Physics 16(20),
500 13309.

501 Han, S., Kondo, Y., Oshima, N., Takegawa, N., Miyazaki, Y., Hu, M., Lin, P., Deng, Z., Zhao, Y.,
502 Sugimoto, N., Wu, Y., 2009. Temporal variations of elemental carbon in Beijing. Journal of
503 Geophysical Research: Atmospheres 114(D23), DOI: 10.1029/2009JD012027.

504 He, K. B., Yang, F. M., Duan, F. K., Ma Y. L., 2011. Atmospheric Particulate Matter and Regional
505 Complex Pollution. Science Press, Beijing, China. 310-327.

506 He, K. B., Yang, F. M., Ma, Y. L., Zhang, Q., Yao, X. H., Chan, C. K., Cadle, S., Chan, T., Mulawa,

P., 2001. The characteristics of $PM_{2.5}$ in Beijing, China. Atmos. Environ. 35: 4959–4970.

Jeong, B., Bae, M. S., Ahn, J., Lee, J., 2017. A study of carbonaceous aerosols measurement in metropolitan area performed during korus-aq 2016 campaign. Journal of Korean Society for Atmospheric Environment, 33.

Ji, D. S., Li, L., Pang, B., Xue, P., Wang, L. L., Wu, Y. F., Zhang, H. L., Wang, Y. S., 2017. Characterization of black carbon in an urban-rural fringe area of Beijing. Environmental Pollution 223, 524-534.

Ji, D. S., Li, L., Wang, Y. S., Zhang, J. K., Cheng, M. T., Sun, Y., Liu, Z. R., Wang, L. L., Tang, G. Q., Hu, B., Chao, N., Wen, T. X., Miao, H. Y., 2014. The heaviest particulate air-pollution episodes occurred in northern China in January, 2013: Insights gained from observation. Atmospheric Environment 92, 546-556.

Ji, D. S., Zhang, J. K., He, J., Wang, X. J., Pang, B., Liu, Z. R., Wang, L. L., Wang, Y. S., 2016. Characteristics of atmospheric organic and elemental carbon aerosols in urban Beijing, China. Atmospheric Environment 125, 293-306.

Keuken, M. P., Jonkers, S., Zandveld, P., Voogt, M., 2012. Elemental carbon as an indicator for evaluating the impact of traffic measures on air quality and health. Atmospheric Environment 61, 1-8.

Kleinman, L. I., Springston, S. R., Daum, P. H., Lee, Y. N., Nunnermacker, L. J., Senum, G. I., Wang, J., Weinstein-Lloyd, J., Alexander, M. L., Hubbe, J., Ortega, J., Canagaratna, M. R., Jayne, J., 2008. The time evolution of aerosol composition over the Mexico City plateau. Atmospheric Chemistry and Physics 8, 1559-1575.

Lin, P., Hu, M., Deng Z, Slanina, J., Han, S., Kondo, Y., Takegawa, N., Miyazaki, Y., Zhao, Y.,

529 Sugimoto, N., 2009. Seasonal and diurnal variations of organic carbon in $PM_{2.5}$ in Beijing
530 and the estimation of secondary organic carbon. Journal of Geophysical Research:
531 Atmospheres 114(D2), DOI: 10.1029/2008JD010902.
532 Lu, Z., Zhang, Q., Streets, D. G., 2011. Sulfur dioxide and primary carbonaceous aerosol
533 emissions in China and India, 1996–2010. Atmospheric Chemistry and Physics 11,
534 9839-9864.
535 Mancilla, Y., Mendoza, A., 2012. A tunnel study to characterize $PM_{2.5}$ emissions from
536 gasoline-powered vehicles in Monterrey, Mexico. Atmospheric environment 59, 449-460.
537 Mauderly, J. L., Chow, J. C., 2008. Health effects of organic aerosols. Inhalation toxicology 20(3),
538 257-288.
539 Miao, L., Liao, X. N., Wang, Y. C., 2016. Diurnal Variation of $PM_{2.5}$ Mass Concentration in
540 Beijing and Influence of Meteorological Factors Based on Long Term Date. Environmental
541 Science, 37(8), 2836-2846.
542 Odum, J., Hoffmann, T., Bowman, F., Collins, R., Flagan, J., Seinfeld, J. H., 1996. Gas/particle
543 partitioning and secondary organic aerosol yields. Environmental Science and Technology 30,
544 2580-2585.
545 Pan, X. L., Kanaya, Y., Wang, Z. F., Liu, Y., Pochanart, P., Akimoto, H., Sun, Y. L., Dong, H. B.,
546 Li, J., Irie, H., Takigawa, M., 2011. Correlation of black carbon aerosol and carbon monoxide
547 in the high-altitude environment of Mt. Huang in Eastern China. Atmospheric Chemistry and
548 Physics 11, 9735-9747.
549 Pan, X. L., Kanaya, Y., Wang, Z. F., Taketani, F., Tanimoto, H., Irie, H., Takashima, H., Inomata,
550 S., 2012. Emission ratio of carbonaceous aerosols observed near crop residual burning
551 sources in a rural area of the Yangtze River Delta Region, China. Journal of Geophysical

552 Research: Atmospheres, 117(D22).
553 Pandis, S. N., Harley, R. A., Cass, G. R., 1992. Secondary organic aerosol formation and transport.
554 Atmospheric Environment Part A. General Topics 26(13), 2269-2282.
555 Polissar, A. V., Hopke, P. K., Paatero, P., Kaufmann, Y. J., Hall, D. K., Bodhaine, B. A., Dutton, E.
556 G., Harris, J. M., 1999. The aerosol at Barrow, Alaska: long-term trends and source locations.
557 Atmospheric Environment 33(16), 2441-2458.
558 Pope III, C. A., Dockery, D. W., 2006. Health effects of fine particulate air pollution: lines that
559 connect. Journal of the air & waste management association 56(6), 709-742.
560 Ren, Z. H., Wan, B. T., Yu, T., Su, F. Q., Zhang, Z. G., Gao, Q. X., Yang, X. X., Hu, H. L., Wu, Y.
561 H., Hu, F., Hong, Z. X., 2004. Influence of Weather System of Different Scales on Pollution
562 Boundary Layer and the Transport in Horizontal Current Field. Research of Environmental
563 Sciences 17(1), 7-13.
564 Schauer, J. J., Kleeman, M. J., Cass, G. R., Simoneit, B. R., 2001. Measurement of emissions from
565 air pollution sources. 3. C1-C29 organic compounds from fireplace combustion of wood.
566 Environmental Science & Technology 35(9), 1716-1728.
567 Schauer, J. J., Kleeman, M. J., Cass, G. R., Simoneit, B. R., 2002. Measurement of emissions from
568 air pollution sources. 5. C1− C32 organic compounds from gasoline-powered motor vehicles.
569 Environmental science & technology 36(6), 1169-1180.
570 Seinfeld, J. H., & Pandis, S. N. (2016). Atmospheric chemistry and physics: from air pollution to
571 climate change. John Wiley & Sons.
572 Seinfeld, J. H., Erdakos, G. B., Asher, W. E., Pankow, J. F., 2001. Modeling the Formation of
573 Secondary Organic Aerosol (SOA). 2. The Predicted Effects of Relative Humidity on Aerosol

574 Formation in the α-Pinene-, β-Pinene-, Sabinene-, Δ^3-Carene-, and Cyclohexene-Ozone
575 Systems. Environmental Science and Technology 35(9), 1806-1817.
576 Singer, B., Kirchstetter, T., Harley, R., Kendall, G., Hesson, J., 1999. A fuel based approach to
577 estimating motor vehicle cold-start emissions. Journal of the Air & Waste Management
578 Association 49(2), 125-135.
579 Sun, Y., Jiang, Q., Wang, Z., Fu, P., Li, J., Yang, T., Yin, Y., 2014. Investigation of the sources and
580 evolution processes of severe haze pollution in Beijing in January 2013. Journal of
581 Geophysical Research: Atmospheres 119(7), 4380-4398.
582 The Intergovernmental Panel on Climate Change (IPCC), Fifth Assessment Report (AR5) 2013.
583 http://www.ipcc.ch/report/ar5/wg1/
584 Wang, Y. Q., Zhang, X. Y., Draxler, R. R., 2009. TrajStat: GIS-based software that uses various
585 trajectory statistical analysis methods to identify potential sources from long-term air
586 pollution measurement data. Environmental Modelling & Software 24(8), 938-939.
587 World Health Organization, 2005. http://apps.who.int/iris/bitstream/10665/69477/1/WHO_SDE_
588 PHE_OEH_06.02_eng.pdf.
589 Wu, D., Liao, B. T., Wu, M., Chen, H. Z., Wang, Y. C., Liao, X. N., Gu, Y., Zhang, X. L., Zhao, X.
590 J., Quan, J. N., Liu, W. D., Meng, J. P., Sun, D., 2014. The long-term trend of haze and fog
591 days and the surface layer transport conditions under haze weather in North China. Acta
592 Scientiae Circumstantiae (in Chinese) 34(1), 1-11.
593 Yao, Q., Zhao, P. S., Han, S. Q., Liu, A. X., 2014. Pollution character of carbonaceous aerosol in
594 $PM_{2.5}$ in Tianjin City. Environmental Chemistry (in Chinese) 33, 404-410.
595 Zhao, P. S., Dong, F., Yang, Y. D., He, D., Zhao, X. J., Zhang, W. Z., Yao, Q., Liu, H. Y., 2013.

596 Characteristics of carbonaceous aerosol in the region of Beijing, Tianjin, and Hebei, China.
597 Atmospheric Environment 71, 389-398.
598 Zheng, G. J., Duan, F. K., Su, H., Ma, Y. L., Cheng, Y., Zheng, B., Zheng, B., Zhang, Q., Huang,
599 T., Kimoto, T., Chang, D., Pöschl, U., Cheng, Y. F., He, K. B., 2015. Exploring the severe
600 winter haze in Beijing: the impact of synoptic weather, regional transport and heterogeneous
601 reactions. Atmospheric Chemistry and Physics 15(6), 2969-2983.

Figure legends

Fig. 1. Map and location of the sampling site (the trapezoidal symbol is the sampling site and the five star symbol is the IAP site).

Fig. 2. The whisker-box plots of OC and EC for each month in 2013 and 2014 (In this study, all legends in the box-whisker plots are the same).

Figs. 3(a) Diurnal cycles of OC and EC during the four seasons. (b) Diurnal cycles of OC and EC on weekdays and weekends during the four seasons.

Fig. 4. The concentrations of OC and EC and the wind sectors of the different seasons of 2013 and 2014.

Fig. 5. The potential source areas for OC and EC varied among the four seasons of 2013 (a) and 2014 (b).

Figure
Click here to download Figure: Figures-1.docx

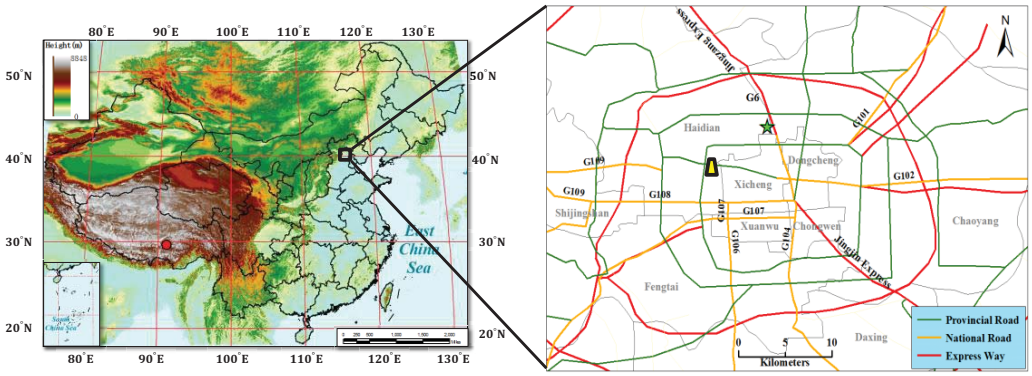

Fig. 1. Map and location of the sampling site (the trapezoidal symbol is the sampling site and the five star symbol is the IAP site).

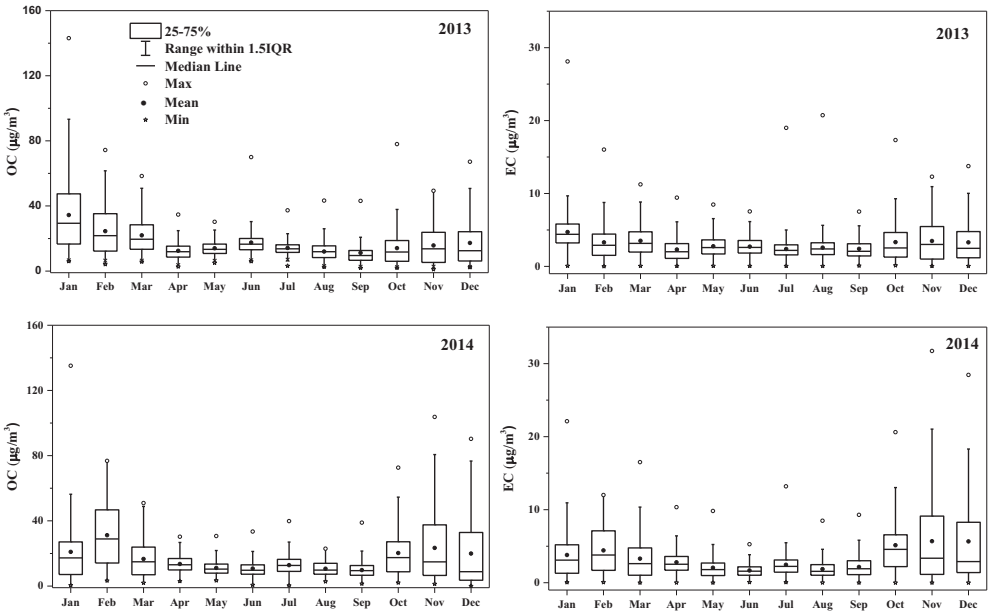

Fig. 2. The whisker-box plots of OC and EC for each month in 2013 and 2014 (In this study, all legends in the box-whisker plots are the same).

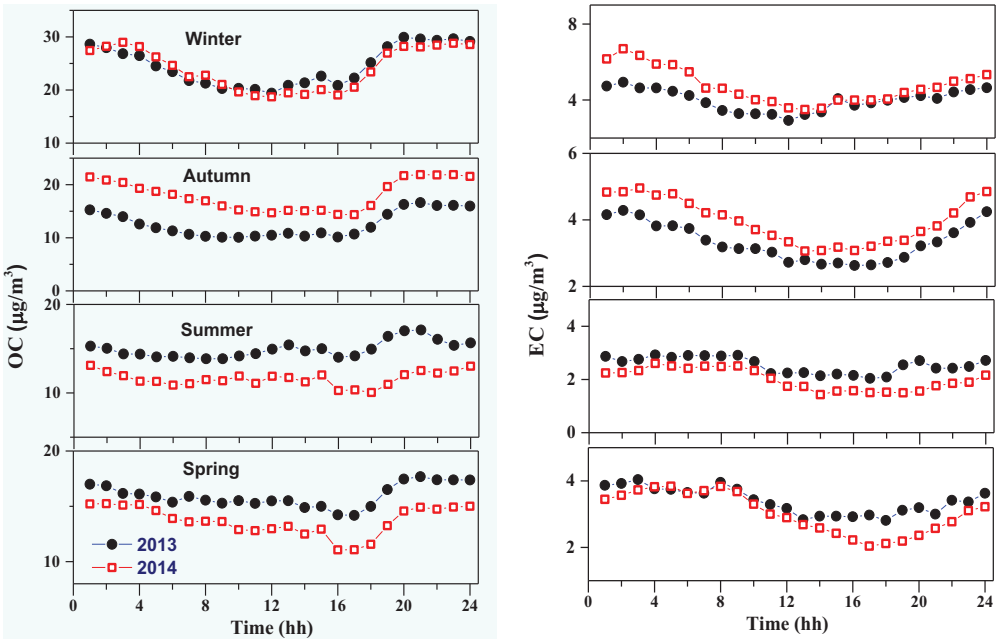

(a)

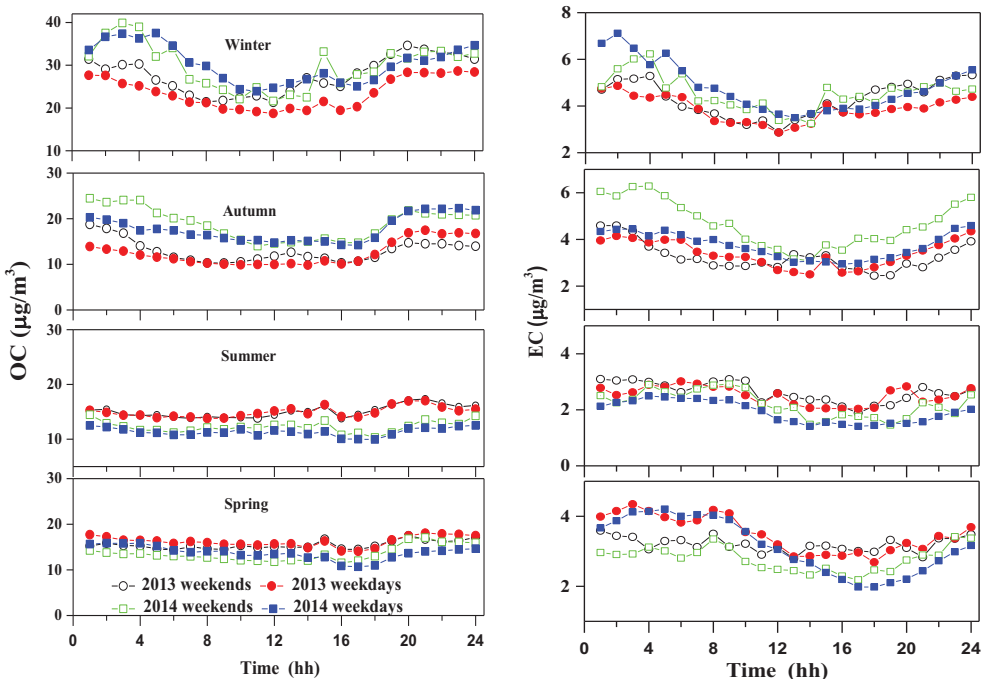

(b)

Figs. 3(a) Diurnal cycles of OC and EC during the four seasons. (b) Diurnal cycles of OC and EC on weekdays and weekends during the four seasons.

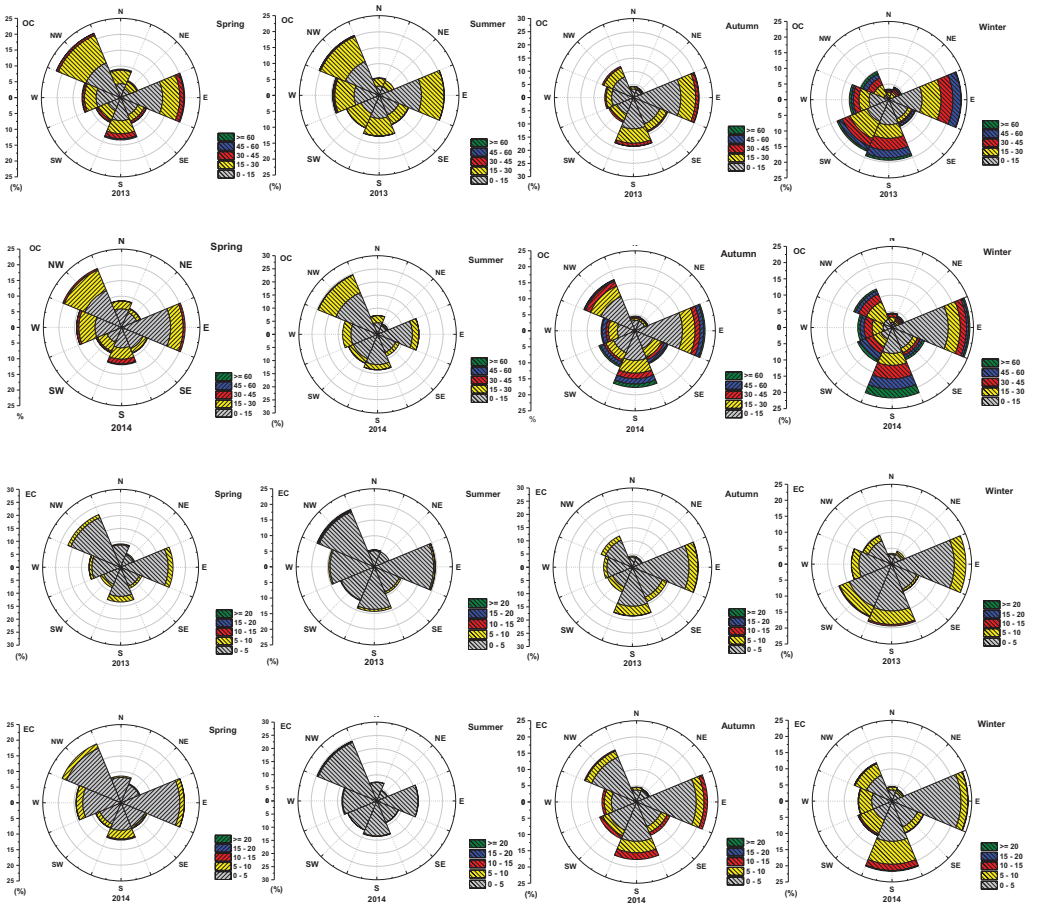

Fig. 4. The concentrations of OC and EC and the wind sectors of the different seasons of 2013 and 2014.

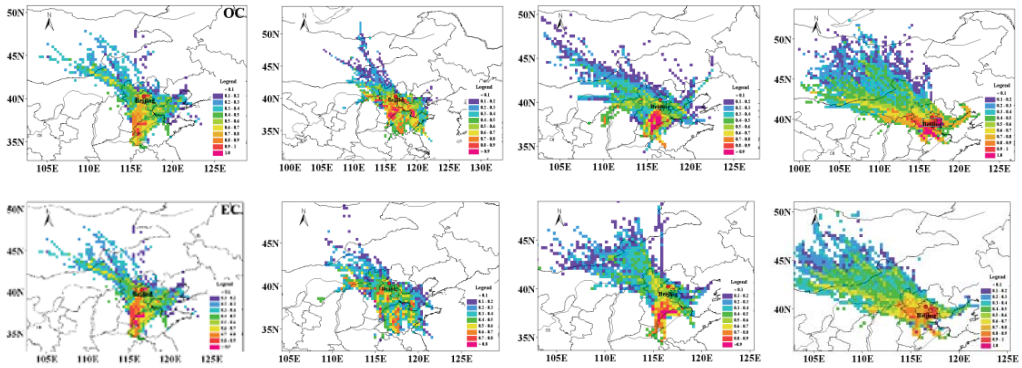

（a）

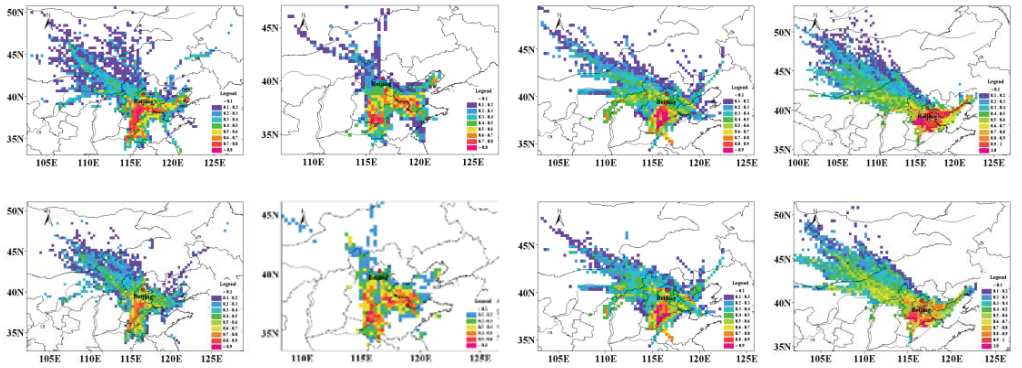

(b)

Fig. 5. The potential source areas for OC and EC varied among the four seasons of 2013 (a) and 2014 (b).

Supplementary Material

Click here to download Supplementary Material: supplementary materials.doc

View publication stats